Safety enhancement, energy analysis and capacity improvement of lithium based batteries

By

USMAN SALAHUDDIN

Reg #: 00000118927

Session 2015-17

Supervised by

Dr. Naseem Iqbal

A Thesis Submitted to the U.S. – Pakistan Cen

ter for Advanced Studies in Energy in partial fulfilment of the requirements for the degree of

MASTERS of SCIENCE in

ENERGY SYSTEMS ENGINEERING

U.S. – Pakistan Center for Advanced Studies in Energy (USPCAS-E)

National University of Sciences and Technology (NUST)

H-12, Islamabad 44000, Pakistan

November 2017

THESIS ACCEPTANCE CERTIFICATE

Certified that final copy of MS/MPhil thesis written by Mr Usman Salahuddin (Registration No. 00000118927), of U.S. – Pakistan Center for Advanced Studies in Energy has been vetted by undersigned, found complete in all respects as per NUST Statues/Regulations, is free of plagiarism, errors, and mistakes and is accepted as partial fulfilment for award of MS degree. It is further certified that necessary amendments as pointed out by GEC members of the scholar have also been incorporated in the said thesis.

Signature:

Name of Supervisor

Date:

Signature (HoD):

Date:

Signature (Dean/Principal):

Date:

Certificate

This is to certify that the work in this thesis has been carried out by Mr. Usman Salahuddin and completed under my supervision in Biofuels Lab, USPCAS-E, NUST, Main Campus, Sector H-12, Islamabad, Pakistan.

Supervisor:

Dr. Naseem Iqbal
USPCAS-E
NUST, Islamabad

GEC Member # 1:

Dr. Muhammad Bilal Khan
USPCAS-E
NUST, Islamabad

GEC Member # 2:

Dr. Eng. Muhammad Zubair
USPCAS-E
NUST, Islamabad

GEC Member # 3:

Dr. Emad Uddin
SMME
NUST, Islamabad

HoD USPCAS-E:

Dr. Zuhair S. Khan
USPCAS-E
NUST, Islamabad

Principal / Dean:

Dr. Muhammad Bilal Khan
USPCAS-E
NUST, Islamabad

Abstract

The main idea of my research is promotion and enhancement of lithium based batteries. One of the objectives of my research was to produce nano-wired copper particles for their possible application in a thermos-responsive polymer switching (TRPS) material, with nano-wired copper particles as the conductive filler, and polyethylene as the base matrix in order to improve the safety parameter of lithium based batteries. At normal operating temperatures the material will exhibit a high electrical conductivity but under circumstances of extreme temperature that may lead to thermal runaway, the material resistance will increase several folds with in a second, thus, saving the battery form thermal runaway and explosion. Furthermore, modification and cyclic voltammetry testing of MOF based cathode materials was performed to propose an optimized cathode material for lithium air batteries. Moreover, I have also worked on the grid to wheel energy efficiency comparison of a fuel cell vehicle with a battery electric vehicle to state the fact that why battery electric vehicles makes more sense in a renewable energy future.

Table of Contents

Table of Figures

List of Tables

Chapter # 1

Introduction

1.1 Renewable Energy Storage

As we move towards a renewable energy economy, our main source of energy production will be solar photovoltaic (PV). Solar PVs' prices have been going down by roughly 22%/2 year for the last couple of decades. But the problem with solar energy is that it is intermittent. The sun does not shine at night. So, we need a storage medium to store energy produced during day to use at night. The best viable option at present is Lithium ion batteries. They have a reasonable energy and power density. They can also be produced at a large scale. The main problems with Lithium ion batteries are their high cost and safety. As we aim to produce batteries with higher and higher energy densities, safety requirements become more stringent. So, I decided to inherit a safety feature internally in the battery material to make them explosion proof. Moreover, lithium-air batteries offer very good theoretical energy densities, the main challenge here is to develop novel electrodes to enhance their stability and actual capacities.

As the world is moving towards a renewable energy economy, we should also start releasing its urgency. A great number of technology entrepreneurs like Elon Musk (CEO Tesla Motors, SpaceX) and highly reputed college professors like Tony Seba (Stanford University) have predicted that by 2030 the all modes of transportation will become electric. So in order to cope up with global change and also to deal with the energy challenges in Pakistan we should also start taking initiatives to move towards an entirely electric transportation system with lithium ion batteries as the primary source of energy storage. This research provides a solution for better and safer Lithium based batteries.

Following are the main objectives covered in this thesis;

- Safety enhancement of Lithium ion batteries.
- Copper nanowires synthesis and oxidation time based analysis.

- Grid to wheel efficiency comparison of Fuel cell vehicles with Battery electric vehicles.
- Synthesis and performance testing of hybrid cathode materials for Lithium air batteries.

1.2 Safer Lithium Ion Batteries

The main components of a LIB are two electrodes, separator and electrolyte. The separators generally used have melting point ranging from 130°C to 160°C [1]. If due to shorting or overcharging a large amount of heat is generated, the battery separator might melt which triggers a series of exothermic reactions leading towards a thermal runaway [2]. To

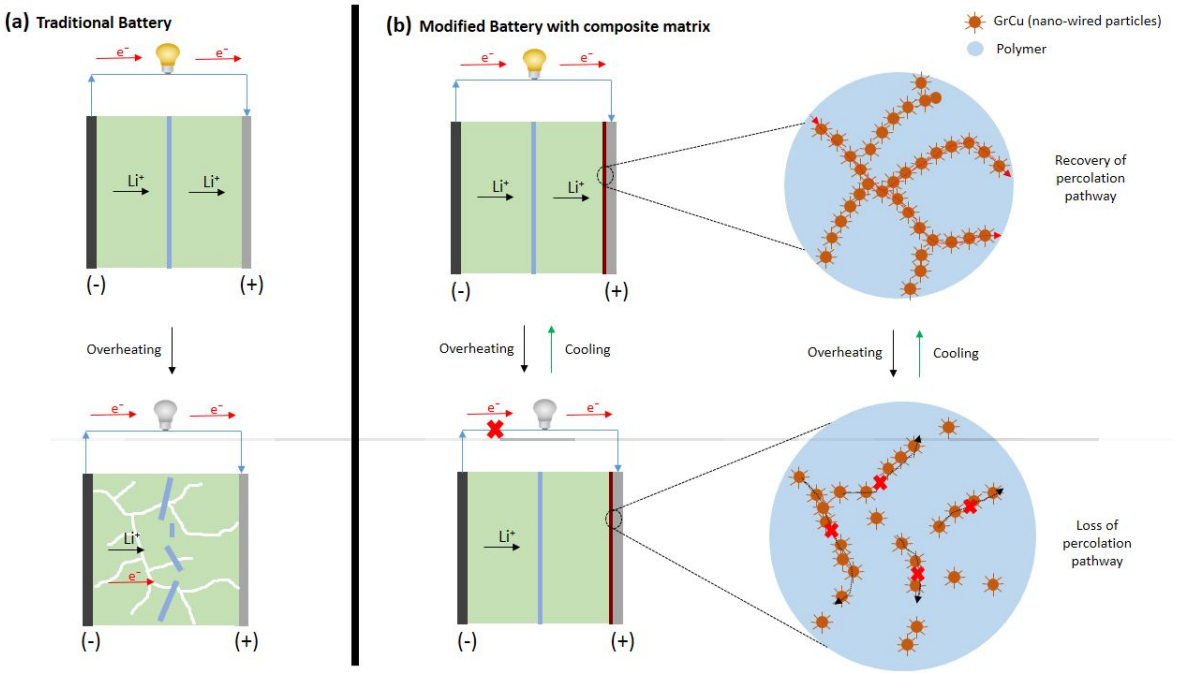

avoid this, we are proposing a design approach that includes an addition of a thermos-responsive polymer switching (TRPS) layer to at least one of the current collectors, forming a hybrid current collector. This TRPS layer works on the principle of quantum tunneling phenomenon. The nano-wired copper particles in this quantum tunneling composite (QTC) material are essential as the nanowires offers enhanced electrical conductivity within the composite matrix as compared to the normal spherical copper particles. This eventually helps in enhancing the conductive percolation [3, 4]. The material offers very low electrical resistance below switching temperature (T_s) but becomes highly insulating above its T_s. As soon as the material achieves its switching temperature, the polymer matrix expands thus breaking the contact between the filler particles and hence increase the overall resistance of

the material. The switching behaviour is explained in Figure 1. The value of T_s can be practically designed according to the requirement by changing the amount of filler particle in the TRPS composite material. The polymer used also effect the switching temperature of the prepared composite matrix.

1.3 Copper Nanoparticles as a Possible Solution

In this research, we report an approach to develop a self-regulating smart material that will be sandwiched between the electrode and current collector. The material consists of conductive carbon coated nano-wired copper particles as the filler embedded in a polymer matrix with a high thermal expansion coefficient. The reason for using nano-wired copper particles is to enhance temperature sensitivity and electrical conductivity. The carbon coating of the particles increases their electrochemical stability once this composite matrix is incorporated within the battery. The as fabricated material will show a good electrical conductivity at room temperature but the conductivity will suddenly drop drastically if the temperature shots beyond a pre-set designed temperature thus preventing the battery from thermal runaway [3]. The material also shows reversible behaviour and hence allows the battery to resume its normal operation once the temperature returns to a normal value.

Moreover, a study was also performed on copper nanoparticles to understand the effect of oxidation time on the size and diameter of nanowires. The length and diameter of these CuO nanowires are in the range of approximately 3-15 μm and 100-300 nm respectively. SEM images of the oxidized copper particles were examined to understand the effect of oxidation time on the length and population density of the nanowire. Oxidation times were set from 15 minutes to 4 hours. We report a direct relation between oxidation time and the population density of the nanowires. An increase in length of the wires was observed up to an oxidation time of 3 hours, however, further increase in oxidation time did not significantly contribute to an increased length of nanowires. XRD and TGA was performed to identify the phases of CuO and oxidation rate of Cu respectively.

1.4 Battery Electric Vehicles vs. Fuel Cell Vehicles

Sustainable energy consumption is as important a part of the renewable energy economy as renewable energy generation and storage. Almost one third of the global energy consumption can be credited to the transportation of goods and people around the globe. In order to move towards a renewable energy based economy, we must adopt to a more sustainable energy consumption pattern worldwide especially in the transportation sector. In this article, a comparison is being made between the energy efficiency of a fuel cell vehicle (FCV) and a battery electric vehicle (BEV). A very simple yet logical approach has been followed to determine the overall energy required by each vehicle. Other factors that hinder the progress of FCV in market are also discussed. Additionally, the prospects of a hydrogen economy are also discussed in detail. The arguments raised in this thesis are based on physics, economic analyses and laws of thermodynamics. It clearly shows that an 'electric economy' makes far greater sense than a 'hydrogen economy'. The main objective of this analysis is to determine the energy efficacy of battery powered vehicles as compared to fuel cell powered vehicles.

1.5 Hybrid Cathode Materials for Lithium Air Batteries

Lithium ion batteries are prospective candidates for energy storage in near future as they offer a very high energy density as compared to lithium ion batteries and almost comparable to gasoline. In lithium air batteries the anode is usually pure lithium metal while oxygen or air is used as cathode material. Different carbon based electrodes are used as cathode to provide reaction sites to oxygen. Platinum has been used widely as a catalyst material with carbon support for Li-air battery cathode but it is highly expensive. In order to address this issue different non noble and transition metals have been used to come up with a cathode that is low cost, stable and offers good energy densities.

The main reaction occurring at the cathode is between oxygen and lithium. Oxygen reduction reaction (ORR) and oxygen evolution reaction (OER) are the reactions occurring during discharge and charge respectively. In order for a material to qualify as a cathode material for Li-Air batteries it must show both ORR and OER capabilities. In other words the material should be redox active.

Metal organic frameworks (MOFs) can act as a good cathode material for Li-Air batteires. ZIF-67 and Fe/MOF derived nano-porous carbons have been used as it is and then further modified to form a hybrid with MnO_2. Their performances were tested using cyclic voltammetry to determine their onset and peak potentials for ORR and OER.

1.6 References

[1] S. S. Zhang, "A review on the separators of liquid electrolyte Li-ion batteries," *Journal of Power Sources,* vol. 164, pp. 351-364, 2007.

[2] P. Balakrishnan, R. Ramesh, and T. P. Kumar, "Safety mechanisms in lithium-ion batteries," *Journal of Power Sources,* vol. 155, pp. 401-414, 2006.

[3] Z. Chen, P.-C. Hsu, J. Lopez, Y. Li, J. W. To, N. Liu*, et al.*, "Fast and reversible thermoresponsive polymer switching materials for safer batteries," *Nature Energy,* vol. 1, p. 15009, 2016.

[4] D. Bloor, A. Graham, E. Williams, P. Laughlin, and D. Lussey, "Metal–polymer composite with nanostructured filler particles and amplified physical properties," *Applied Physics Letters,* vol. 88, p. 102103, 2006.

Chapter # 2

Copper Nanoparticles

2.1 Introduction

Metal oxide nanowires have been getting increasing attention due to their wide variety of applications like their use in energy harvesting, electronics, sensors and photonics [1-4]. Their unique properties like photon and phonon confinement, one dimensionality and optical functionality have made them suitable for these and a lot of other applications [5]. Among metal oxide nanowires, copper oxide nanowires have become a topic of special interest pertaining to their high thermal and electrical conductivities, localized effects and quantized conductance [6, 7]. Application for these nanowires range from heat transfer and solar cells to semiconductor devices and conductive adhesives [8]. Additionally, copper oxide has delivered best oxidation/reduction performance for chemical combustion of solid coal [9]. It has also been successfully used as an excellent catalyst in methane and carbon monoxide combustion [10, 11].

A variety of methods have been previously reported to synthesize copper oxide nanowires including vapor-liquid-solid (VLS) method [12], template-directed method [13], epitaxial growth {Zhou, 2008 #97}[14], in situ-resolved X-ray diffraction [15, 16] and chemical vapor deposition . However, some of these methods involve intricate processes, complex equipment, and expensive raw materials and offer limited scalability while other methods involve sophisticated template removal techniques that further add to the cost and effort of producing nanowires. Few of the methods even involve reducing agents like hydrazine that is extremely toxic in nature [17, 18].

A much simple, cost effective and scalable method for the synthesis of copper oxide nanowires is the thermal oxidation of copper substrates in any form like foils, wires, grids [19-22]. Sintered copper particles have been frequently used for heat transfer applications [8,

23-25]. Moreover it has been formerly reported that suitable particle size, porosity and structure of the particles can help enhance heat transfer [25, 26].

In this work, we have fabricated copper oxide nanowires from copper particles. Although, effects of different oxidation temperatures and particle size on the morphology of the nanowires have been previously reported [27, 28] but the effect of the oxidation time on the length and population density of the nanowires has still been an overlooked area. To achieve this goals, copper particles were sintered using six different time profiles to understand the effects of oxidation time on the morphology of the nanowires.

2.2 Experimental method

5 g sample of spherical copper powder (Alfa Aesar) with a particle size range between 10-50 μm, evenly distributed on a flat silicon substrate, was placed in a box furnace. Appropriate temperature for nanowires growth has been reported to be between 400-700°C [20, 21]. The temperature of the furnace was pre-set to a suitable value of 600°C. Ambient air flow was maintained throughout all the experiments. The particles were then sintered in the furnace at 600°C for 15 minutes. The experiment was repeated for 30 minutes, 1, 2, 3 and 4 hours under same conditions.

After oxidation, the particles were carefully scrapped from the silicon substrate without damaging the nanowires. Scanning Electron Microscopy (SEM - VEGA3) images of the oxidized particles were then observed to understand the effect of varying time on the length of the nanowires. Energy dispersive Spectroscopy was also used to confirm the conversion of copper into copper oxide. Thermo gravimetric analysis (TGA) was performed with ambient air flow on the nano-wired particles to obtain oxidation rate. Percent gain in weight was noted against time at a fixed temperature of 600°C for almost an hour. Moreover, X-ray Diffraction (XRD - D8 Advanced Diffractometer) was performed to understand the crystal structure of the nanowires.

2.3 Results and Discussions

Oxidation of spherical copper powder under different time profiles resulted in different surface morphologies of copper particles. At and below 30 minutes of oxidation, no

nanowires on the surface of the particles were observed, while we did observe nanowires at and above an oxidation time of 1 hours. Nanowires were found to be almost perpendicular to the surface of the particles and no entanglement or even branching of the wires was detected. Interesting to observe was an increase in the average length of the nanowires with increasing oxidation time. The oxidation temperature was fixed to an optimum value of 600°C [28]. Furthermore, particles after oxidation were found to be hollow from inside, possibly due to an effect called Kirkendall effect [29].

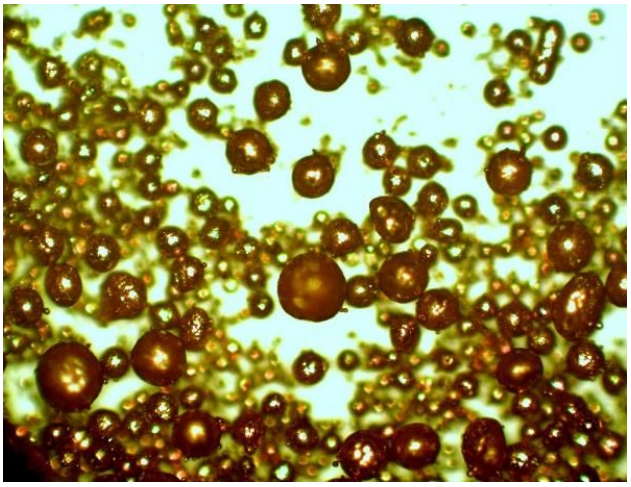

Figure 3 Spherical Copper particles under optical microscope

At first, copper particles were heated at 600°C for 15 minutes under ambient air conditions. SEM images of the oxidized particles are shown in Figure 2. No nanowires were observed after 15 minutes of oxidation.

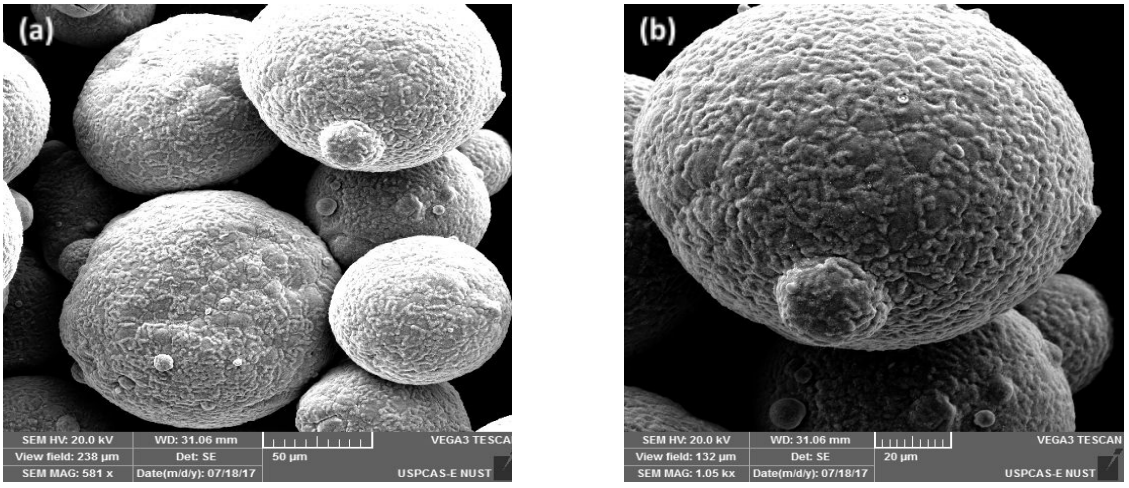

Figure 4 CuO with an oxidation time of 15 minutes

Copper powder was then oxidized using the same conditions, except oxidation time was increased to 30 minutes this time, however, no nanowires were observed even this time as shown in Figure 3. Copper simply converted to copper oxide as confirmed through EDS.

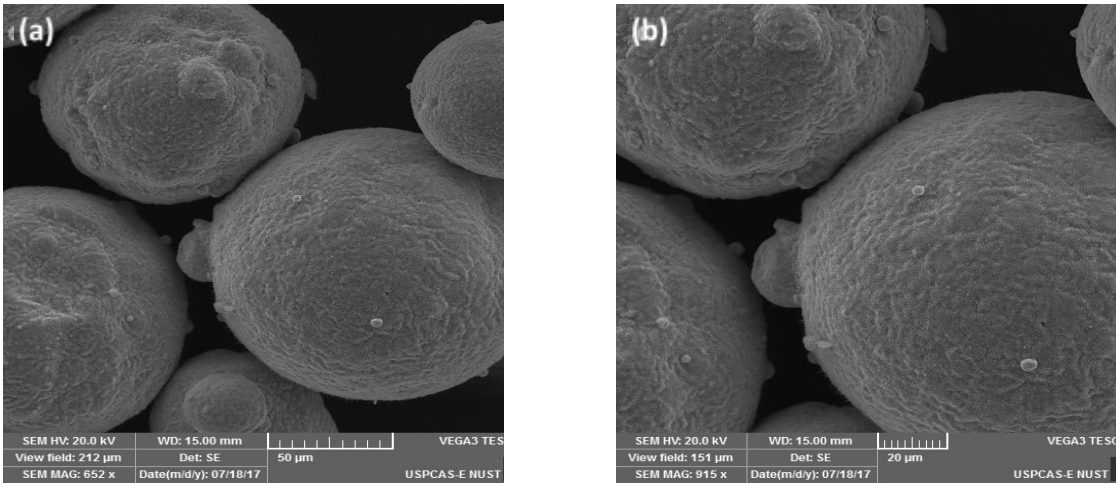

Figure 5. CuO with an oxidation time of 30 minutes

When the Copper particles were allowed an oxidation time of 1 hour, nanowires did form perpendicular to the surfaces of the particles as shown in Figure 4.

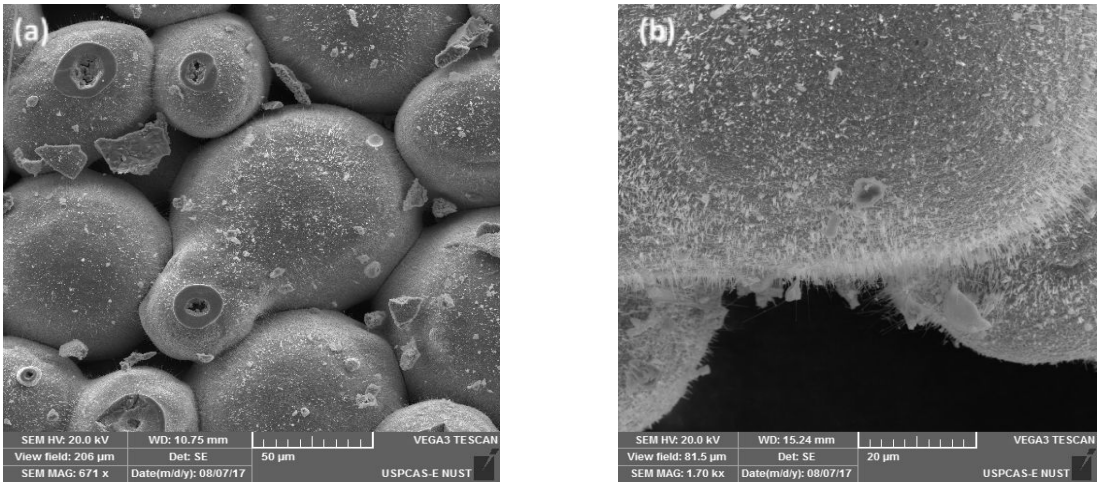

Figure 6. CuO nanowires with an oxidation time of 1 hour

Subsequently, Cu powder was once again thermally oxidized by changing the oxidation to 2 and 3 hours respectively. An increase in the average length of the nanowires was observed. Similarly, an increase in population density of the nanowires was also observed. Copper oxidized for 1 hour had the least number of nanowires relative to the ones

oxidized for 2 and 3 hours. Moreover, copper oxidized for 3 hours had more nanowires on the surface of the particle than that oxidized for 2 hours.

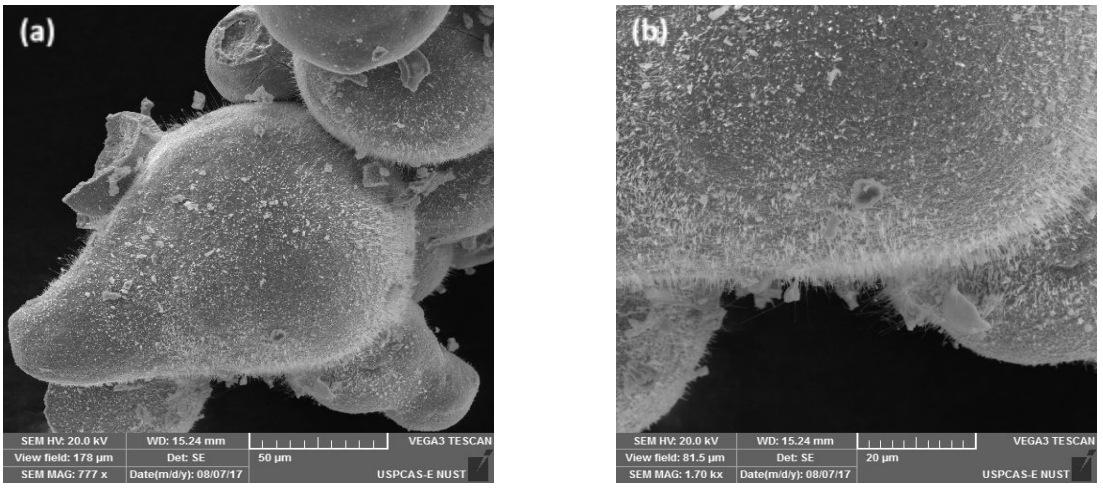

Figure 7. CuO nanowires with an oxidation time of 2 hours

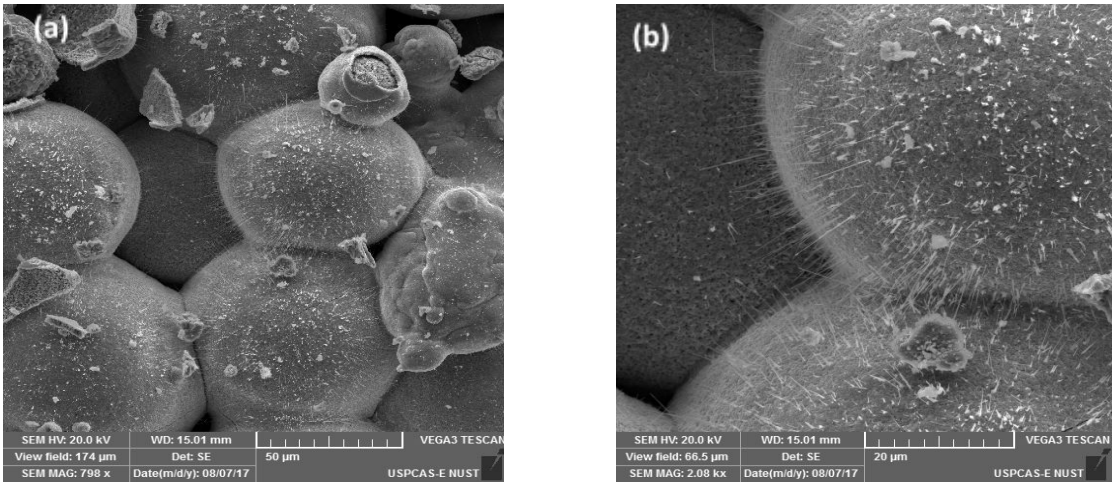

Figure 8. CuO nanowires with an oxidation time of 3 hours

Finally, the sample was oxidized for 4 complete hours. An increase in the population density of the nanowires was observed, however, there was no significant increase in the length of nanowires relative to the sample oxidized for 3 hours. SEM images of Cu powder oxidized for 4 hours are shown in Figure 7. The particle in figure 7(a) appears to be cracked due to handling during removal from the silicon substrate. The images clearly show a marked increase in the number of nanowires formed.

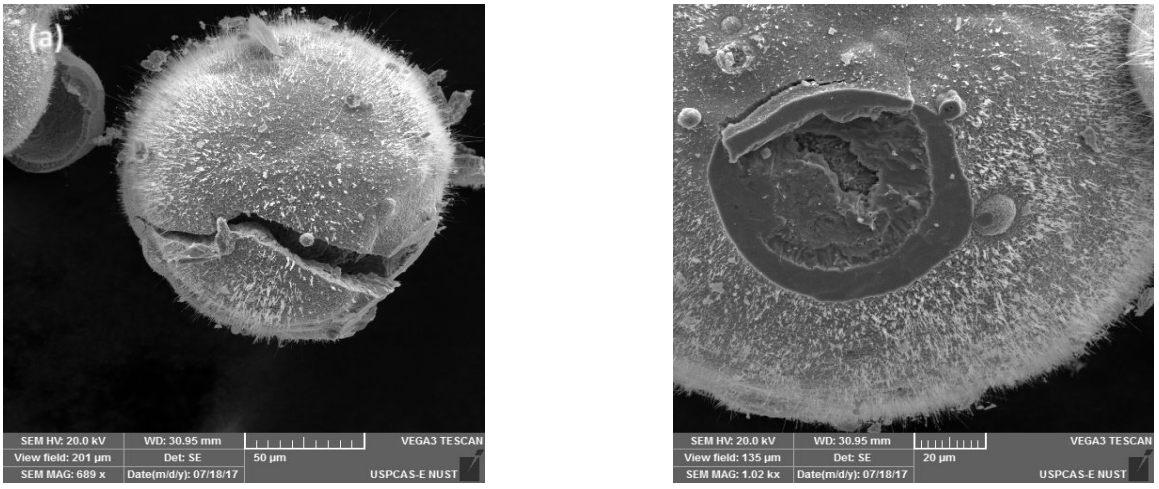

Figure 9. CuO nanowires with an oxidation time of 4 hours

The average length of the nanowires were calculated by measuring length of multiple wires (by using scaling tools on SEM on high resolution SEM images) at multiples points as well as multiple particles with in the sample as shown in . The approximate lengths of the particles were found to be in the range from 3-10 µm while diameter of the particles were found to be in the range of 100-300 nm.

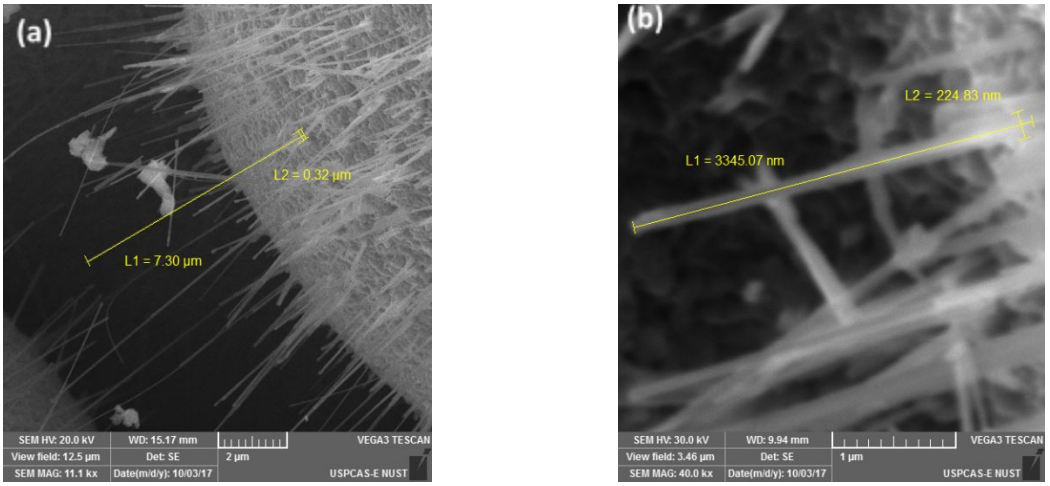

Figure 10. Length and diameter determination of CuO nanowires

Evident from these SEM images is an increasing trend for the length of the nanowires formed. As the oxidation time was increased, the length of the wires also increased. However, above a certain oxidation time, there is no further noticeable increase in the length of these nanowires. Additionally, population density of nanowires increased proportional to the increase in oxidation time. Figure 9 below distinctly exhibits an increase in population density of nanowires with increasing time.

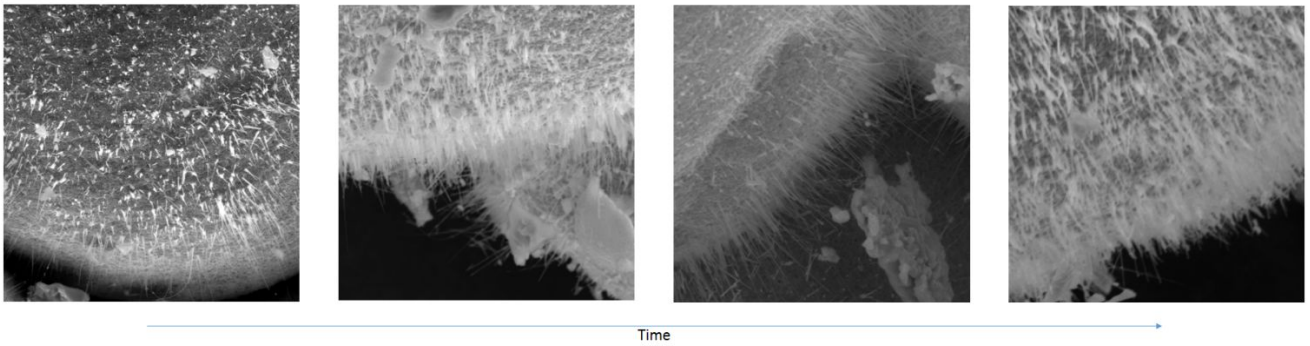

Figure 11. Sequential SEM images of copper oxide nanowires with different oxidation time profiles; (a) 1 hour, (b) 2 hours, (c) 3 hours, (d) 4 hours

Eventually, EDS of the nano-wired copper oxide particles was performed to confirm the conversion of most of the copper in CuO or Cu_2O.

Table 1 clearly shows that ~62% (atomic %) of the sample is oxygen, which ensures the conversion of copper the CuO and Cu_2O.

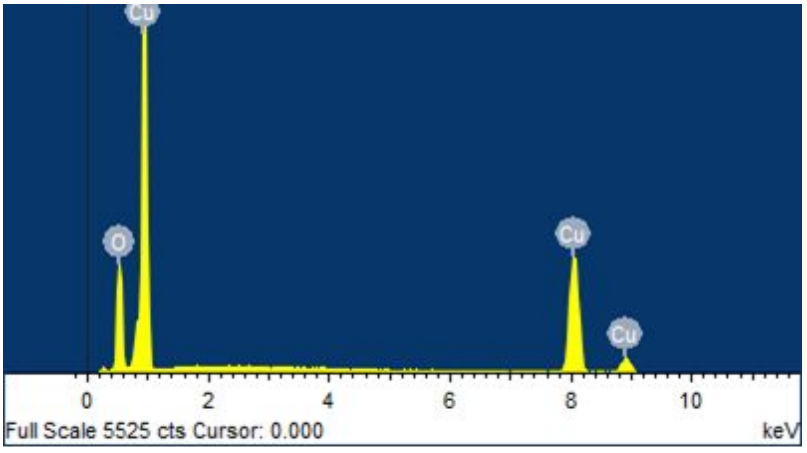

Table 1. Average atomic weight percentages of elements in oxidized samples

Element	Atomic weight (%)
Cu	38.51
O	61.49
Total	100

Figure 11 shows the increase in weight percent as copper in turned in to copper oxide with time. The graph shows a linear trend which represents that the amount of copper oxide and hence population density of nanowires increases with increasing time.

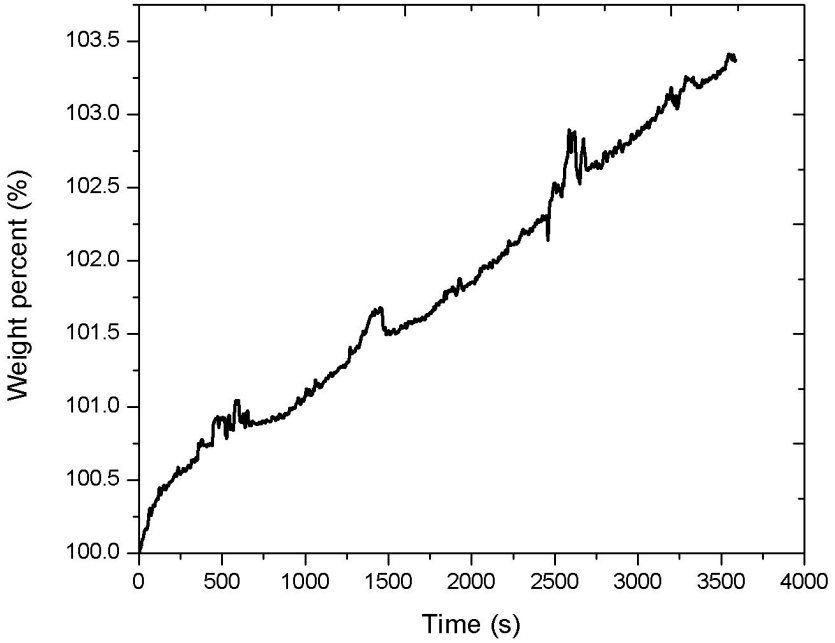

Figure 13. TGA analysis of Cu particles at 600 °C showing increasing trend in weight percent with time

XRD analysis of the CuO particles with nanowires confirmed presence of CuO as the major phase while copper and cuprite was also detected. This confirms conversion of most of the copper into copper oxide and thus the nanowires formed are also composed of copper oxide. The XRD pattern of nano-wired particles exhibited the characteristic peaks of CuO (Tenorite, syn, PDF#48-1548), Cu (copper, syn, PDF#04-0836) and cuprite (cuprite, syn, PDF#05-0667) respectively. From the PDF card, the suggested crystal structure for CuO nanowires was monoclinic.

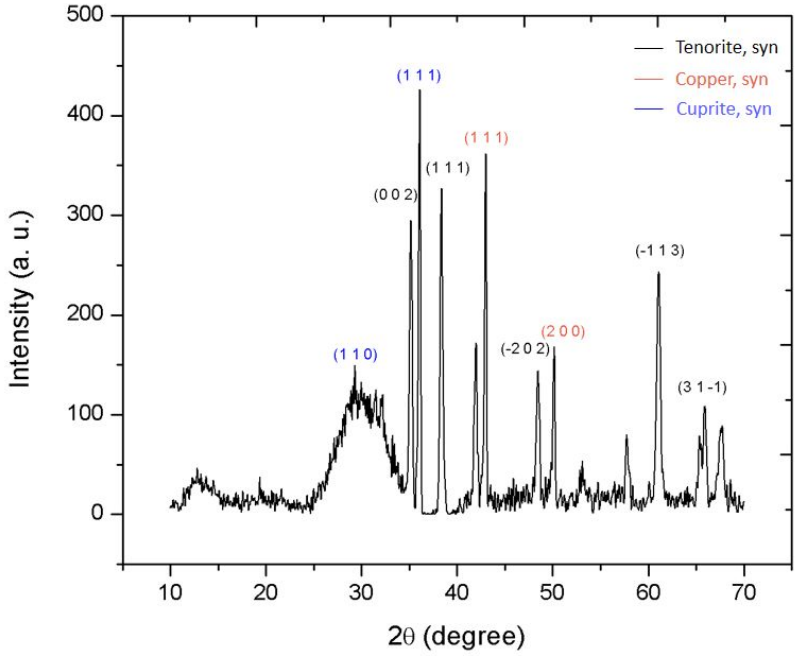

Figure 14. XRD peaks of copper nano-wired particles

Finally, this study clearly developed a coherent relationship between oxidation time and the length and population density of nanowires. Understanding the effect of different parameters on the nature and shape of these nanowires will help us better optimize their potential use in applications like heat transfer, catalysis, electronics cooling, etc.

2.4 Conclusion

Conclusively, an oxidation time based analysis was performed on the population densities and lengths of nanowires. The greatest length observed was for the sample oxidized for 3 hours while no further increase in length of wires was observed beyond that oxidation time. Additionally, no nanowires were observed at or below an oxidation temperature of 30 minutes. The population density was greatest for copper with a given oxidation time of 4 hours. Three hours is the optimum time to achieve the longest nanowires. Moreover, nanowires formed perpendicular to the surfaces of the particles without any entanglement or branching. EDS results were used to confirm conversion of copper to copper while TGA results proved enhanced oxidation of copper with time. Finally, XRD results confirmed that the crystal structure of the nanowires formed is monoclinic. The length of the nanowires is in the range of 3-10 μm while the diameter of the nanowires lies in the range of 100-300 nm.

2.5 References

[1] Z. L. Wang and J. Song, "Piezoelectric nanogenerators based on zinc oxide nanowire arrays," *Science,* vol. 312, pp. 242-246, 2006.

[2] P.-C. Chen, G. Shen, H. Chen, Y.-g. Ha, C. Wu, S. Sukcharoenchoke*, et al.*, "High-performance single-crystalline arsenic-doped indium oxide nanowires for transparent thin-film transistors and active matrix organic light-emitting diode displays," *ACS nano,* vol. 3, pp. 3383-3390, 2009.

[3] M. C. McAlpine, H. Ahmad, D. Wang, and J. R. Heath, "Highly ordered nanowire arrays on plastic substrates for ultrasensitive flexible chemical sensors," *Nature materials,* vol. 6, p. 379, 2007.

[4] R. Yan, D. Gargas, and P. Yang, "Nanowire photonics," *Nature photonics,* vol. 3, pp. 569-576, 2009.

[5] P. Yang, R. Yan, and M. Fardy, "Semiconductor nanowire: what's next?," *Nano letters,* vol. 10, pp. 1529-1536, 2010.

[6] D. Zhang, R. Wang, M. Wen, D. Weng, X. Cui, J. Sun*, et al.*, "Synthesis of ultralong copper nanowires for high-performance transparent electrodes," *Journal of the American Chemical Society,* vol. 134, pp. 14283-14286, 2012.

[7] M. Meyyappan and M. K. Sunkara, *Inorganic nanowires: applications, properties, and characterization*: CRC Press, 2009.

[8] H. P. J. de Bock, K. Varanasi, P. Chamarthy, T. Deng, A. Kulkarni, B. M. Rush*, et al.*, "Experimental investigation of micro/nano heat pipe wick structures," in *ASME 2008 International Mechanical Engineering Congress and Exposition*, 2008, pp. 991-996.

[9] R. Siriwardane, H. Tian, G. Richards, T. Simonyi, and J. Poston, "Chemical-looping combustion of coal with metal oxide oxygen carriers," *Energy & Fuels,* vol. 23, pp. 3885-3892, 2009.

[10] Y. Feng, P. M. Rao, D. R. Kim, and X. Zheng, "Methane oxidation over catalytic copper oxides nanowires," *Proceedings of the Combustion Institute,* vol. 33, pp. 3169-3175, 2011.

[11] Y. Feng and X. Zheng, "Plasma-enhanced catalytic CuO nanowires for CO oxidation," *Nano letters,* vol. 10, pp. 4762-4766, 2010.

[12] T. J. Trentler, K. M. Hickman, S. C. Goel, A. M. Viano, P. C. Gibbons, and W. E. Buhro, "Solution-liquid-solid growth of crystalline III-V semiconductors: an analogy to vapor-liquid-solid growth," *Science,* pp. 1791-1794, 1995.

[13] Y. Xia, P. Yang, Y. Sun, Y. Wu, B. Mayers, B. Gates*, et al.*, "One-dimensional nanostructures: synthesis, characterization, and applications," *Advanced materials,* vol. 15, pp. 353-389, 2003.

[14] H. Zhou and S. S. Wong, "A facile and mild synthesis of 1-D ZnO, CuO, and α-Fe2O3 nanostructures and nanostructured arrays," *Acs Nano,* vol. 2, pp. 944-958, 2008.

[15] J. A. Rodriguez, J. Y. Kim, J. C. Hanson, M. Pérez, and A. I. Frenkel, "Reduction of CuO in H 2: in situ time-resolved XRD studies," *Catalysis Letters,* vol. 85, pp. 247-254, 2003.

[16] H. Choi and S.-H. Park, "Seedless growth of free-standing copper nanowires by chemical vapor deposition," *Journal of the American Chemical Society,* vol. 126, pp. 6248-6249, 2004.

[17] E. Vernot, J. MacEwen, R. Bruner, C. Haun, E. Kinkead, D. Prentice*, et al.*, "Long-term inhalation toxicity of hydrazine," *Fundamental and Applied Toxicology,* vol. 5, pp. 1050-1064, 1985.

[18] J. K. Niemeier and D. P. Kjell, "Hydrazine and aqueous hydrazine solutions: evaluating safety in chemical processes," *Organic Process Research & Development,* vol. 17, pp. 1580-1590, 2013.
[19] P. M. Rao and X. Zheng, "Rapid catalyst-free flame synthesis of dense, aligned α-Fe2O3 nanoflake and CuO nanoneedle arrays," *Nano letters,* vol. 9, pp. 3001-3006, 2009.
[20] C. Xu, C. H. Woo, and S. Shi, "Formation of CuO nanowires on Cu foil," *Chemical Physics Letters,* vol. 399, pp. 62-66, 2004.
[21] X. Jiang, T. Herricks, and Y. Xia, "CuO nanowires can be synthesized by heating copper substrates in air," *Nano Letters,* vol. 2, pp. 1333-1338, 2002.
[22] J. Chen, F. Zhang, J. Wang, G. Zhang, B. Miao, X. Fan*, et al.*, "CuO nanowires synthesized by thermal oxidation route," *Journal of Alloys and Compounds,* vol. 454, pp. 268-273, 2008.
[23] G. P. Peterson, "An introduction to heat pipes: modeling, testing, and applications," 1994.
[24] M. Kaviany, "Principles of Heat Transfer in Porous Media, Springer, New York, 1995."
[25] J. A. Weibel, S. V. Garimella, and M. T. North, "Characterization of evaporation and boiling from sintered powder wicks fed by capillary action," *International Journal of Heat and Mass Transfer,* vol. 53, pp. 4204-4215, 2010.
[26] S. G. Liter and M. Kaviany, "Pool-boiling CHF enhancement by modulated porous-layer coating: theory and experiment," *International Journal of Heat and Mass Transfer,* vol. 44, pp. 4287-4311, 2001.
[27] N. M. Rashid, N. Kishi, and T. Soga, "Effects of reduction temperature on copper nanowires growth by thermal reduction of copper oxide nanowires," *Modern Physics Letters B,* vol. 30, p. 1650193, 2016.
[28] C. J. Love, J. D. Smith, Y. Cui, and K. K. Varanasi, "Size-dependent thermal oxidation of copper: single-step synthesis of hierarchical nanostructures," *Nanoscale,* vol. 3, pp. 4972-4976, 2011.
[29] E. Mel, M. Buffière, P. Y. Tessier, S. Konstantinidis, W. Xu, K. Du*, et al.*, "Highly ordered hollow oxide nanostructures: the kirkendall effect at the nanoscale," *Small,* vol. 9, pp. 2838-2843, 2013.

Chapter # 3

Thermo-responsive polymer switching material

3.1 Introduction

Metal oxide nanowires [1] have found increasing application in the recent years in the fields of nano-electronics [2], energy harvesting [3], heat transfer[4, 5] etc. Nanowires offer a high surface to volume ratio, good electrical and thermal properties. Copper being one the most commonly available metal has become the preferred material of choice for the synthesis of modified nano-wired particles[6]. Methods currently used for the synthesis of such nanowires include chemical vapor deposition [7], complex emulsion assisted hydrothermal process [8, 9], electrochemical deposition [10, 11], template directed and epitaxial growth [12, 13]. However, a very simple yet salable approach is thermal oxidation of spherical copper particles [14, 15]. A very practical application of copper nanowires is its use in the fabrication of a thermo-responsive polymer switching (TRPS) material to improve the safety parameter of Lithium ion batteries.

Furthermore, electric vehicles, consumer electronics and stationary energy storage demands reliable and safe Lithium ion batteries (LIBs) [16-18]. Although energy as well as power densities of such batteries have been drastically improved in the past two decades, safety has been relatively an overlooked issue. With rising interest in increasing the energy densities of the current lithium ion batteries, safety is one of the primary factor that is impeding the wide scale disruption of lithium ion batteries in the market.

Lithium ion batteries normally operate within a pre-defined range of voltage, current and temperature. However, a series of abnormal exothermic reactions can initiate, like a negative feedback loop, most likely due to overcharging, physical abuse or shorting, leading towards cataclysmic fire or sometimes even explosion [19, 20]. To prevent such failures, LIBs are usually equipped with external positive coefficient (PTC) resistors and pressure

release vents to avoid overheating and overpressure respectively. Nevertheless, such external temperature and pressure control devices lag in detecting a sudden surge in temperature inside the cell [21]. This calls for strategies that can detect such temperature surges from within the cells.

A number of different approaches have been used to address the safety issue internally. Using electrolyte additives, PTC modified current collectors and advanced separators have been found useful but they all have some limitations. Various novel separator approaches, like thermos-responsive microspheres [22], ceramic coating of particles [23, 24] and bilayer or tri-layer [25, 26] separators, do help in stopping current flow at undesired elevated temperatures but all these techniques are irreversible which means that the battery becomes nonfunctional afterwards. On the other hand, electrolyte additives like redox shuttles [27-30], flame retardants [31, 32] suffer from the problem of low operating voltage range and poor cyclic stability. Moreover, nonflammable solid electrolytes might solve such safety problems but they drastically reduce battery performance rendering to their low ionic conductivities [33-40]. Use of PTC modified current collectors is another viable option but their room temperature conductivities are quite low and they also suffer from high leakage current problem [21, 41]. Evident from the limitations above is the need for a new approach to effectively address the current LIBs safety problem.

In this research, we report an approach to develop a self-regulating smart material that will be sandwiched between the electrode and current collector. The material consists of conductive carbon coated nano-wired copper particles as the filler embedded in a polymer matrix with a high thermal expansion coefficient. The reason for using nano-wired copper particles is to enhance temperature sensitivity and electrical conductivity. The carbon coating of the particles increases their electrochemical stability once this composite matrix is incorporated within the battery. The as fabricated material will show a good electrical conductivity at room temperature but the conductivity will suddenly drop drastically if the temperature shoots beyond a pre-set designed temperature thus preventing the battery from thermal runaway [42]. The material also shows reversible behavior and hence allows the battery to resume its normal operation once the temperature returns to a normal value.

3.2 Experimentation

Spherical copper (~ 10g) particles were heated to temperature of 600°C for one hour in a tube furnace under normal atmospheric air flow using a silicon substrate. The oxidized particles were then reduced in the same tube furnace using a hydrogen (10%) and argon (90%) flow through the tube. The temperature was maintained at 400°C for 2 hours. The reduced particles were mixed with ethanol and gently stirred with a magnetic stirrer for almost 6 hours to segregate the particles clumped together due to heating process. Once segregated, particles were dried using a vacuum oven.

As the material is to be incorporated in LIBs as part of the polymer composite material, the particles were coated with carbon to improve their electrochemical stability. A dissolution precipitation method was used to coat amorphous carbon on the as fabricated particles as described in the article [42].

A simple yet logical approach was used to fabricate the TRPS matrix. Spherical copper particles (10-50μm, Alfa Aesar) were dispersed in the polyethylene (Sigma Aldrich) using melt flow method with a ratio of 40% (v/v) of copper particles. A thin film of the composite material was formed on a conductive glass piece using doctor blade and later sandwiched between two conductive glass pieces. The thickness of the film was approximately 500 micrometers. Resistance of the material was later plotted against two variables time and temperature respectively.

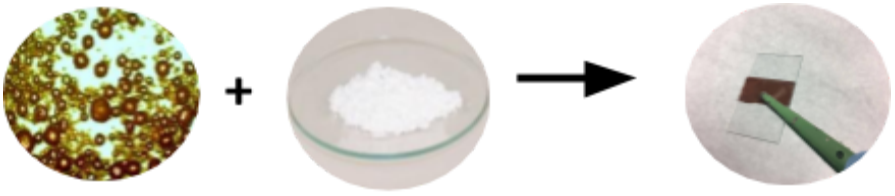

Figure SEQ Figure * ARABIC 15. Synthesis of TRPS film between conducting glass pieces

For resistance testing, the material sandwiched between two conducting glass pieces was connected to an electrical circuit with wires connecting opposite ends of the glass pieces. The circuit includes the glass- composite material- glass sandwich, an LED light and a switch in series. The setup was also connected with a thermocouple, a multi-meter. A stop watch

was used to measure time. As the circuit was connected and the switch was turned on the LED (light emitting diode) simultaneously turned on. Then, heat was supplied through a hot air blower, as the temperature increased the resistance of the material increased with time but the LED still remained lit.

Similarly, the QTC composite can also be synthesized using nano-wired copper particles instead of spherical copper particles to enhance electrical conductivity and switching response of the material.

3.3 Results and Discussions

Thermal oxidation of spherical copper particles (10-50) resulted in formation of nanowires on the surfaces of the particles. Growth of nanowires is a function of time, temperature and also the particle size [14, 15]. The lengths of the wires were in the range of 10-15 μm while their diameters were between 100-200nm. SEM images of the nano-wired particles are shown below in Figure 6. CuO nanowires were then reduced to obtain Cu nanowires. The diameter of the reduced wires is a little less than the oxidized ones. The wires grow perpendicular to the surface of the individual particles which enhance the electrical conductivity at the tips of the nano-wires. The wires also helps to improve the contact between the individual particles due to their increased surface to volume ratio.

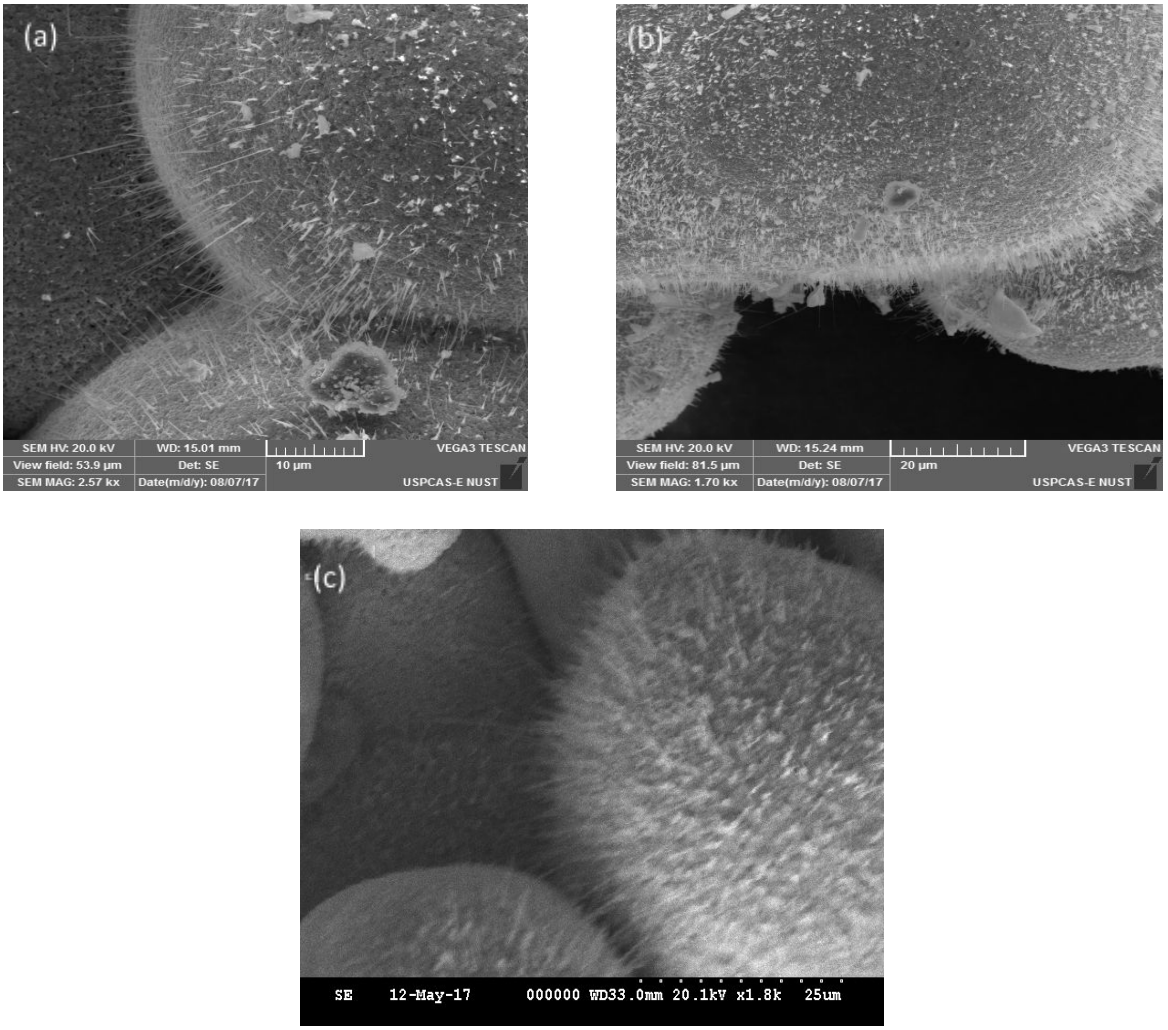

Figure 16. (a), (b) - CuO nano-wired particles, (c) - Cu nano-wired particles

An excellent application for these nano-wired particles is their use in the fabrication of a modified polymer composite to be used as TRPS material in Lithium ion batteries. These wires helps to improve the switching behavior of the composite matrix (relative to the use spherical copper particles in the polymer matrix) due to increased surface area and better contact between the individual particles. Before their use in LIBs, these particles should first be coated with carbon to provide electrochemical stability while avoiding electrolyte decomposition during battery operation. Hence, the nano-wired particles were coated with carbon to enhance electrochemical stability of the composite matrix. The dissolution precipitation was used to coat carbon on the particles. As shown in the Figure 7, the G (~ 1580 cm^{-1}) and D (~1330 cm^{-1}) peaks confirms carbon coating. The ID/IG (where ID and IG are D and G peak intensities) ratio was found to be 0.89.

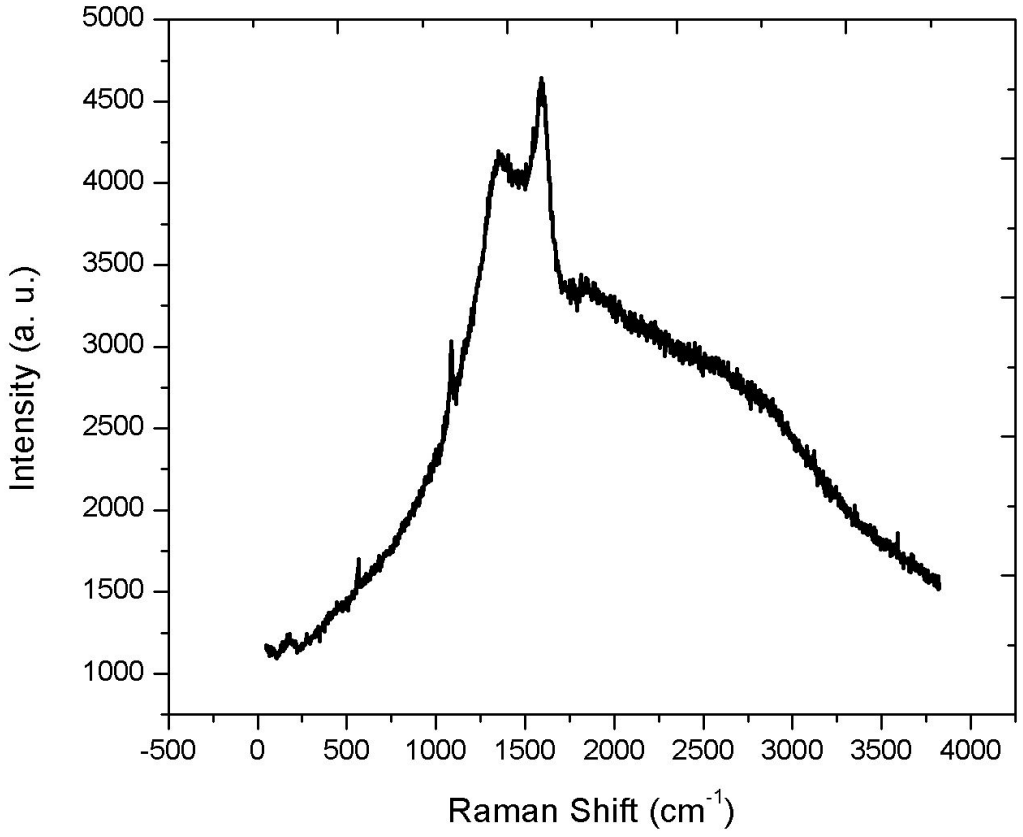

The main components of a LIB are two electrodes, separator and electrolyte. The separators generally used have melting point ranging from 130°C to 160°C [25]. If due to shorting or overcharging a large amount of heat is generated, the battery separator might melt which triggers a series of exothermic reactions leading towards a thermal runaway [26]. To avoid this, we are proposing a design approach that includes an addition of a

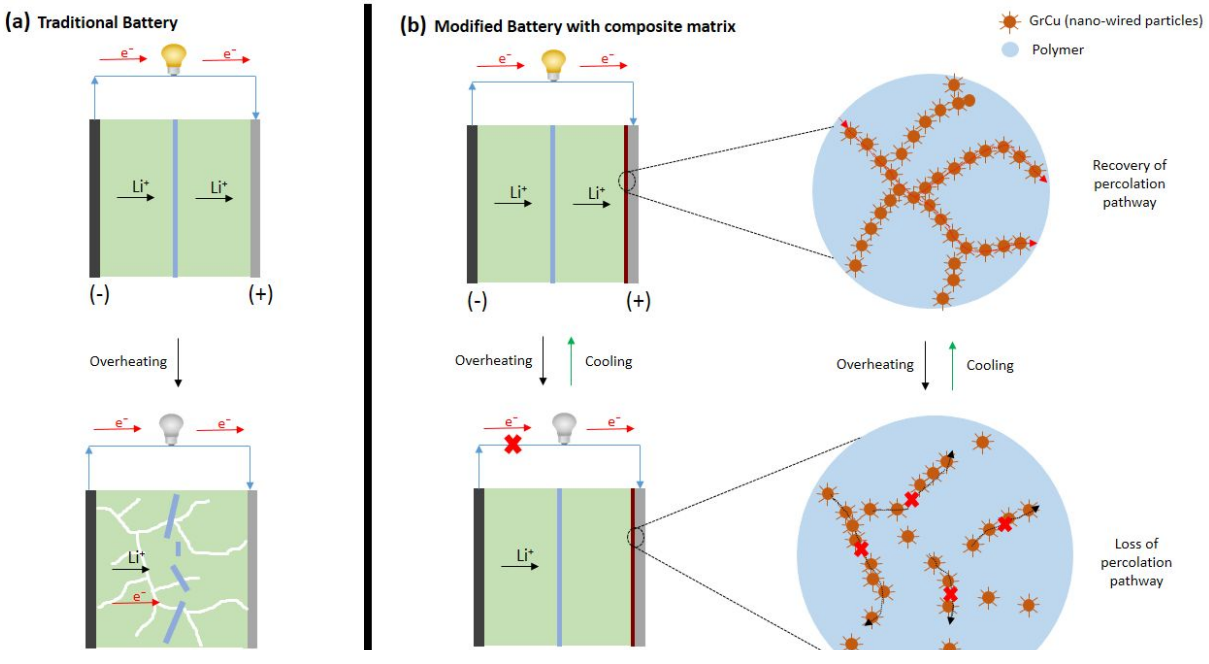

thermos-responsive polymer switching (TRPS) layer to at least one of the current collectors, forming a hybrid current collector. This TRPS layer works on the principle of quantum tunneling phenomenon. The nano-wired copper particles in this quantum tunneling composite (QTC) material are essential as the nanowires offers enhanced electrical conductivity within the composite matrix as compared to the normal spherical copper particles. This eventually helps in enhancing the conductive percolation [42, 43]. The material offers very low electrical resistance below switching temperature (T_s) but becomes highly insulating above its T_s. As soon as the material achieves its switching temperature, the polymer matrix expands thus breaking the contact between the filler particles and hence increase the overall resistance of the material. The switching behavior is explained in Figure 1. The value of T_s can be practically designed according to the requirement by changing the amount of filler particle in the TRPS composite material. The polymer used also effect the switching temperature of the prepared composite matrix.

Figure 18. Switching behavior of the TRPS film incorporated with in a battery

The composite material is primarily made from two components, namely; a metal filler and a polymer binder. A good choice for the polymer binder is polyethylene as it is quite inexpensive, offers high thermal expansion coefficient and a good melt flow index. For the selection of metal filler, a comparative analysis was performed among the most commonly available metals. Copper seemed to be the appropriate choice as shown in Table 1.

	Zinc	***Aluminum***	***Nickel***	***Copper***
Electrical resistivity	✓✓	✓✓	✓✓✓	✓✓✓✓

Thermal Conductivity	✓✓	✓✓✓	✓	✓✓✓✓
Price	✓✓✓	✓✓✓✓	✓✓	✓✓✓
Voltage Stability	✓	✓✓✓	✓✓✓	✓✓

Table 2 Comparison of different metals for filler selection

At first, the composite matrix was simply tested for its resistance with time and temperature as variables. At a temperature of 54°C, the LED suddenly turned off. This temperature can be referred to as the switching temperature of the material. As the heat is removed, the resistance decreased and the LED light turned on again at the switching temperature of the material that was observed earlier. The experiment was repeated 4-5 times and switching was observed at the same temperature. Eventually, a time versus resistance graph was plotted for the composite. The distance between the electrodes for resistance measurement was set to be 1 inch. The pattern observed, as shown in the Figure 3, does show a switching behavior at a fixed switching temperature but the change is resistance is not a step function of time rather it shows a gradual increase and decrease in resistance over time as the heat supply is turned on or off respectively. The LED turned on and off approximately at a resistance of 7kΩ.

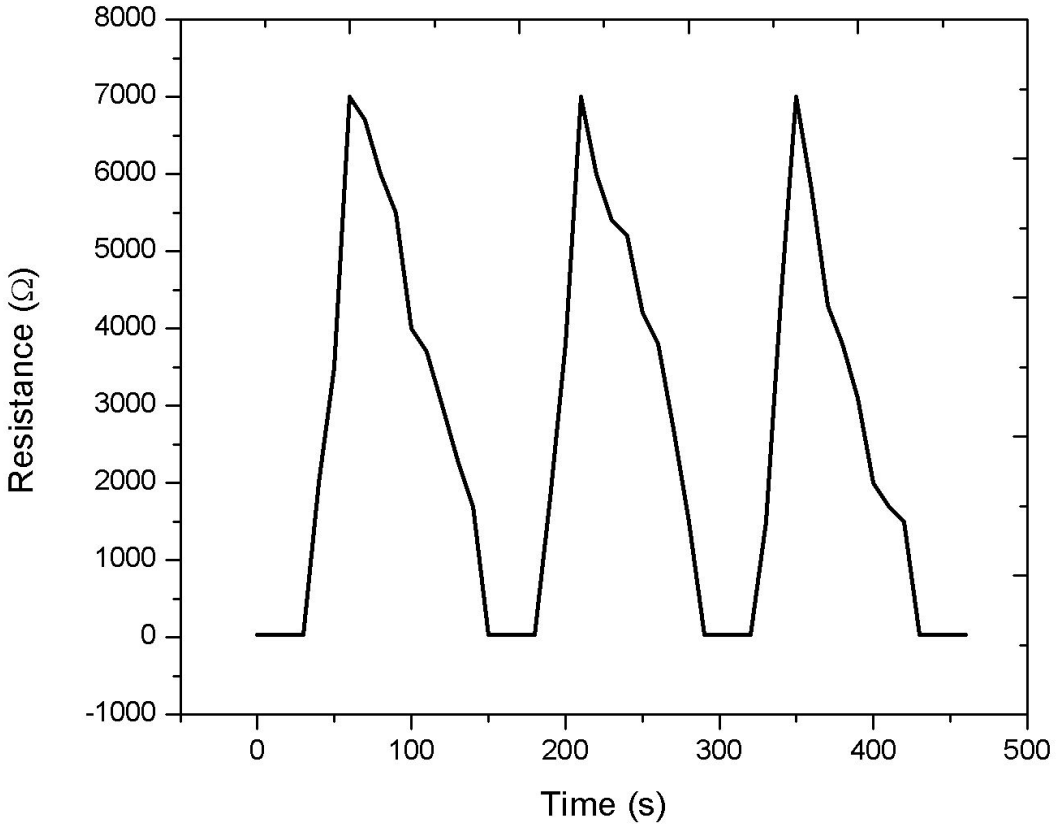

Figure 19. Switching behavior of polymer composite (with spherical copper)

Figure 4 shows the behavior of the ideal QTC composite. The resistance value in this composite changes abruptly following a switching function at a particular preset switching temperature, thereby providing the desired functionality for battery application.

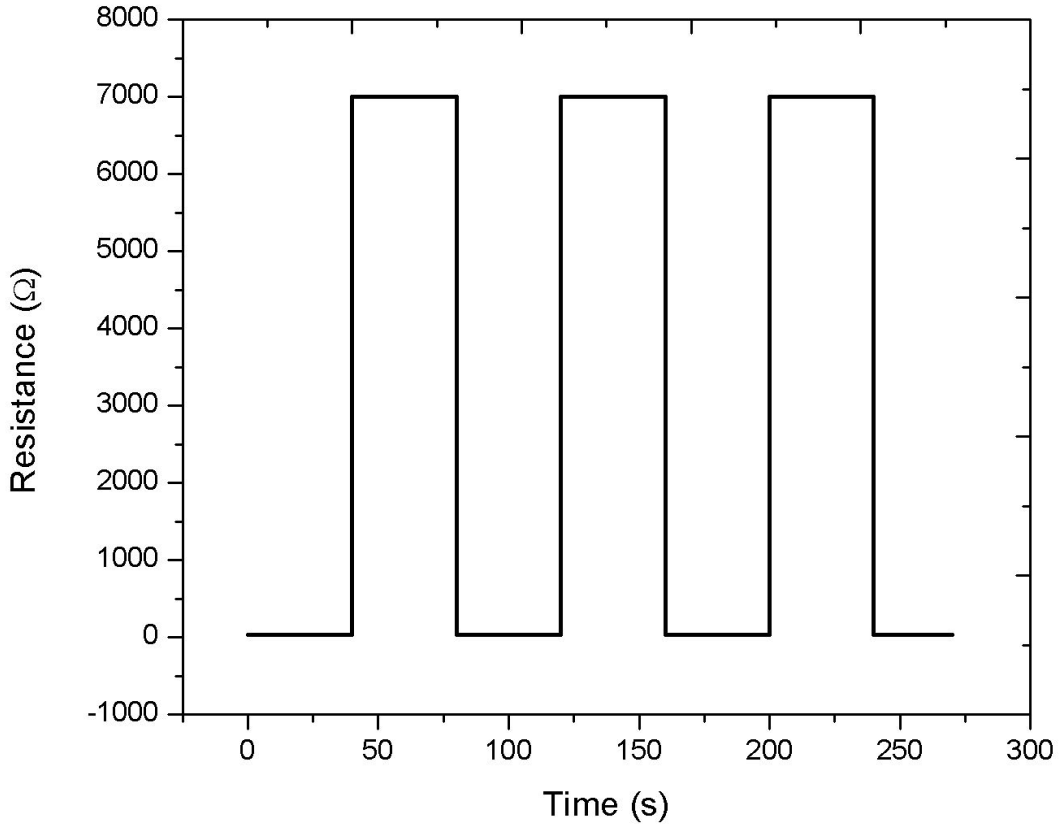

Figure 20. Desired switching behavior of QTC composite

Another graph shown below in Figure 5 shows the relation between resistance and temperature for the composite material synthesized. The graph shows that as temperature increases, the resistances also increases. One important thing to notice from this graph is the rapid change is the slope of the graph at 54°C, which is actually the switching temperature of the material as physically observed.

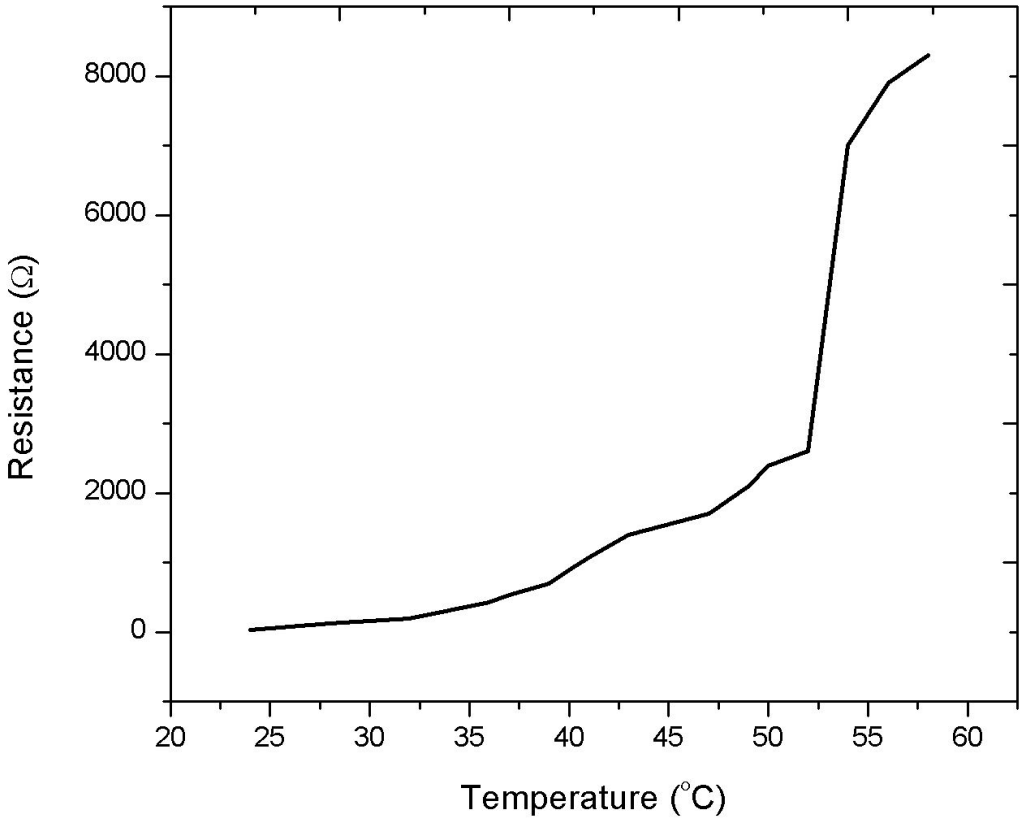

Figure 21. Change in Resistance with respect to temperature

3.4 Conclusion

To summarize, a novel approach has been reported to modify copper particles into nano-wired copper particles to address the safety issue in lithium ion batteries. The wires on the surface of the particles helps to increase localized electrical conductivity by offering a high localized conductivity on their tips. These nano-wired particles were later coated with carbon to improve their electrochemical stability owing to their application within LIBs. Thermal runaway in LIBs can be avoided by using a thermos-responsive polymer switching material within the batteries. The material safely switches the battery off, through thermal expansion of the polymer matrix, by greatly increasing the resistivity of the polymer matrix by many times above its switching temperature. One notable feature of this material is its reversible operation allowing the battery to switch on and off multiple times without affecting

the performance of the battery. Additionally, nano-wired copper particles can be used in fabrication of the TRPS material to further enhance its electrical conductivity and switching behaviour.

3.5 References

[1] P. Yang, R. Yan, and M. Fardy, "Semiconductor nanowire: what's next?," *Nano letters,* vol. 10, pp. 1529-1536, 2010.

[2] P.-C. Chen, G. Shen, H. Chen, Y.-g. Ha, C. Wu, S. Sukcharoenchoke*, et al.*, "High-performance single-crystalline arsenic-doped indium oxide nanowires for transparent thin-film transistors and active matrix organic light-emitting diode displays," *ACS nano,* vol. 3, pp. 3383-3390, 2009.

[3] Z. L. Wang and J. Song, "Piezoelectric nanogenerators based on zinc oxide nanowire arrays," *Science,* vol. 312, pp. 242-246, 2006.

[4] H. P. J. de Bock, K. Varanasi, P. Chamarthy, T. Deng, A. Kulkarni, B. M. Rush*, et al.*, "Experimental investigation of micro/nano heat pipe wick structures," in *ASME 2008 International Mechanical Engineering Congress and Exposition*, 2008, pp. 991-996.

[5] U. Salahuddin, M. Bilal, and H. Ejaz, "A review of the advancements made in helical baffles used in shell and tube heat exchangers," *International Communications in Heat and Mass Transfer,* vol. 67, pp. 104-108, 2015.

[6] D. Zhang, R. Wang, M. Wen, D. Weng, X. Cui, J. Sun*, et al.*, "Synthesis of ultralong copper nanowires for high-performance transparent electrodes," *Journal of the American Chemical Society,* vol. 134, pp. 14283-14286, 2012.

[7] H. Choi and S.-H. Park, "Seedless growth of free-standing copper nanowires by chemical vapor deposition," *Journal of the American Chemical Society,* vol. 126, pp. 6248-6249, 2004.

[8] Y. Shi, H. Li, L. Chen, and X. Huang, "Obtaining ultra-long copper nanowires via a hydrothermal process," *Science and Technology of Advanced Materials,* vol. 6, pp. 761-765, 2005.

[9] R. Wang and H. Ruan, "Synthesis of copper nanowires and its application to flexible transparent electrode," *Journal of Alloys and Compounds,* vol. 656, pp. 936-943, 2016.

[10] Y. Zhao, Y. Zhang, Y. Li, and Z. Yan, "Soft synthesis of single-crystal copper nanowires of various scales," *New Journal of Chemistry,* vol. 36, pp. 130-138, 2012.

[11] H. Cao, L. Wang, Y. Qiu, and L. Zhang, "Synthesis and I–V properties of aligned copper nanowires," *Nanotechnology,* vol. 17, p. 1736, 2006.

[12] Y. Xia, P. Yang, Y. Sun, Y. Wu, B. Mayers, B. Gates*, et al.*, "One-dimensional nanostructures: synthesis, characterization, and applications," *Advanced materials,* vol. 15, pp. 353-389, 2003.

[13] H. Zhou and S. S. Wong, "A facile and mild synthesis of 1-D ZnO, CuO, and α-Fe2O3 nanostructures and nanostructured arrays," *Acs Nano,* vol. 2, pp. 944-958, 2008.

[14] C. J. Love, J. D. Smith, Y. Cui, and K. K. Varanasi, "Size-dependent thermal oxidation of copper: single-step synthesis of hierarchical nanostructures," *Nanoscale,* vol. 3, pp. 4972-4976, 2011.

[15] N. M. Rashid, N. Kishi, and T. Soga, "Effects of reduction temperature on copper nanowires growth by thermal reduction of copper oxide nanowires," *Modern Physics Letters B,* vol. 30, p. 1650193, 2016.

[16] B. Dunn, H. Kamath, and J.-M. Tarascon, "Electrical energy storage for the grid: a battery of choices," *Science,* vol. 334, pp. 928-935, 2011.

[17] N. S. Choi, Z. Chen, S. A. Freunberger, X. Ji, Y. K. Sun, K. Amine*, et al.*, "Challenges facing lithium batteries and electrical double-layer capacitors," *Angewandte Chemie International Edition,* vol. 51, pp. 9994-10024, 2012.

[18] J. B. Goodenough and K.-S. Park, "The Li-ion rechargeable battery: a perspective," *Journal of the American Chemical Society,* vol. 135, pp. 1167-1176, 2013.

[19] D. P. Finegan, M. Scheel, J. B. Robinson, B. Tjaden, I. Hunt, T. J. Mason*, et al.*, "In-operando high-speed tomography of lithium-ion batteries during thermal runaway," *Nature communications,* vol. 6, 2015.

[20] Q. Wang, P. Ping, X. Zhao, G. Chu, J. Sun, and C. Chen, "Thermal runaway caused fire and explosion of lithium ion battery," *Journal of power sources,* vol. 208, pp. 210-224, 2012.

[21] X. Feng, X. Ai, and H. Yang, "A positive-temperature-coefficient electrode with thermal cut-off mechanism for use in rechargeable lithium batteries," *Electrochemistry Communications,* vol. 6, pp. 1021-1024, 2004.

[22] M. Baginska, B. J. Blaiszik, R. J. Merriman, N. R. Sottos, J. S. Moore, and S. R. White, "Autonomic Shutdown of Lithium-Ion Batteries Using Thermoresponsive Microspheres," *Advanced Energy Materials,* vol. 2, pp. 583-590, 2012.

[23] Y. S. Jung, A. S. Cavanagh, L. Gedvilas, N. E. Widjonarko, I. D. Scott, S. H. Lee*, et al.*, "Improved Functionality of Lithium-Ion Batteries Enabled by Atomic Layer Deposition on the Porous Microstructure of Polymer Separators and Coating Electrodes," *Advanced Energy Materials,* vol. 2, pp. 1022-1027, 2012.

[24] J.-A. Choi, S. H. Kim, and D.-W. Kim, "Enhancement of thermal stability and cycling performance in lithium-ion cells through the use of ceramic-coated separators," *Journal of Power Sources,* vol. 195, pp. 6192-6196, 2010.

[25] S. S. Zhang, "A review on the separators of liquid electrolyte Li-ion batteries," *Journal of Power Sources,* vol. 164, pp. 351-364, 2007.

[26] P. Balakrishnan, R. Ramesh, and T. P. Kumar, "Safety mechanisms in lithium-ion batteries," *Journal of Power Sources,* vol. 155, pp. 401-414, 2006.

[27] C. Buhrmester, J. Chen, L. Moshurchak, J. Jiang, R. L. Wang, and J. Dahn, "Studies of aromatic redox shuttle additives for LiFePO4-based Li-ion cells," *Journal of the Electrochemical Society,* vol. 152, pp. A2390-A2399, 2005.

[28] Z. Chen, Y. Qin, and K. Amine, "Redox shuttles for safer lithium-ion batteries," *Electrochimica Acta,* vol. 54, pp. 5605-5613, 2009.

[29] L. Zhang, Z. Zhang, H. Wu, and K. Amine, "Novel redox shuttle additive for high-voltage cathode materials," *Energy & Environmental Science,* vol. 4, pp. 2858-2862, 2011.

[30] L. Zhang, Z. Zhang, P. C. Redfern, L. A. Curtiss, and K. Amine, "Molecular engineering towards safer lithium-ion batteries: a highly stable and compatible redox shuttle for overcharge protection," *Energy & Environmental Science,* vol. 5, pp. 8204-8207, 2012.

[31] Y. E. Hyung, D. R. Vissers, and K. Amine, "Flame-retardant additives for lithium-ion batteries," *Journal of power sources,* vol. 119, pp. 383-387, 2003.

[32] H. Xiang, H. Xu, Z. Wang, and C. Chen, "Dimethyl methylphosphonate (DMMP) as an efficient flame retardant additive for the lithium-ion battery electrolytes," *Journal of Power Sources,* vol. 173, pp. 562-564, 2007.

[33] R. Bouchet, S. Maria, R. Meziane, A. Aboulaich, L. Lienafa, J.-P. Bonnet*, et al.*, "Single-ion BAB triblock copolymers as highly efficient electrolytes for lithium-metal batteries," *Nature materials,* vol. 12, p. 452, 2013.

[34] R. Chen, F. Wu, L. Li, X. Qiu, and S. Chen, "Binary Molten Salt Electrolytes Based on LiClO~ 4 and 2-oxazolidinone," *ACTA PHYSICOCHIMICA SINICA,* vol. 23, p. 554, 2007.

[35] A. Ghosh, C. Wang, and P. Kofinas, "Block copolymer solid battery electrolyte with high Li-ion transference number," *Journal of the electrochemical society,* vol. 157, pp. A846-A849, 2010.

[36] G. Liu, C. L. Reeder, X. Sun, and J. B. Kerr, "Diffusion coefficients in trimethyleneoxide containing comb branch polymer electrolytes," *Solid state ionics,* vol. 175, pp. 781-783, 2004.

[37] D. H. Wong, J. L. Thelen, Y. Fu, D. Devaux, A. A. Pandya, V. S. Battaglia*, et al.*, "Nonflammable perfluoropolyether-based electrolytes for lithium batteries," *Proceedings of the National Academy of Sciences,* vol. 111, pp. 3327-3331, 2014.

[38] K. Xu, S. Zhang, J. L. Allen, and T. R. Jow, "Nonflammable electrolytes for Li-ion batteries based on a fluorinated phosphate," *Journal of The Electrochemical Society,* vol. 149, pp. A1079-A1082, 2002.

[39] X.-W. Zhang, C. Wang, A. J. Appleby, and F. E. Little, "Characteristics of lithium-ion-conducting composite polymer-glass secondary cell electrolytes," *Journal of power sources,* vol. 112, pp. 209-215, 2002.

[40] G. Liu, M. Reinhout, B. Mainguy, and G. L. Baker, "Synthesis, structure, and ionic conductivity of self-assembled amphiphilic poly (methacrylate) comb polymers," *Macromolecules,* vol. 39, pp. 4726-4734, 2006.

[41] J. Li, J. Chen, H. Lu, M. Jia, L. Jiang, Y. Lai*, et al.*, "A positive-temperature-coefficient layer based on Ni-mixed poly (vinylidene fluoride) composites for LiFePO4 electrode," *Int. J. Electrochem. Sci,* vol. 8, pp. 5223-5231, 2013.

[42] Z. Chen, P.-C. Hsu, J. Lopez, Y. Li, J. W. To, N. Liu*, et al.*, "Fast and reversible thermoresponsive polymer switching materials for safer batteries," *Nature Energy,* vol. 1, p. 15009, 2016.

[43] D. Bloor, A. Graham, E. Williams, P. Laughlin, and D. Lussey, "Metal–polymer composite with nanostructured filler particles and amplified physical properties," *Applied Physics Letters,* vol. 88, p. 102103, 2006.

Chapter # 4

Efficiency comparison of EVs

4.1 Introduction

Today's world is addicted to fossil fuels. More specifically oil is the primary source of energy in the transportation sector. More than 60% of the oil produced each day is consumed in transportation sector and more than 96% of the transportation sector's demands are met by liquid fossil fuels [1]. Hence, transition from a fossil fuel economy to a more sustainable renewable energy economy seems like one of the most pressing issues mankind is facing presently. A renewable energy economy model consists of three essential parts mainly; renewable energy generation, energy storage and sustainable energy consumption. While we are well aware about the renewable energy generation through different renewable resources like photovoltaic panels, wind turbines, geothermal resources, etc., the storage of the so generated energy in batteries, capacitors, flywheels, phase change materials, etc., still sustainable energy consumption remains a hardly discussed topic. Light duty passenger vehicles represent almost 60-70% of the carbon dioxide emissions in the transport sector [2]. This paper mainly deals with sustainable energy consumption related to transportation sector, more specifically electric vehicles. The way we decide to proceed towards a renewable energy future and the way we decide to consume energy is surely going to impact our energy future.

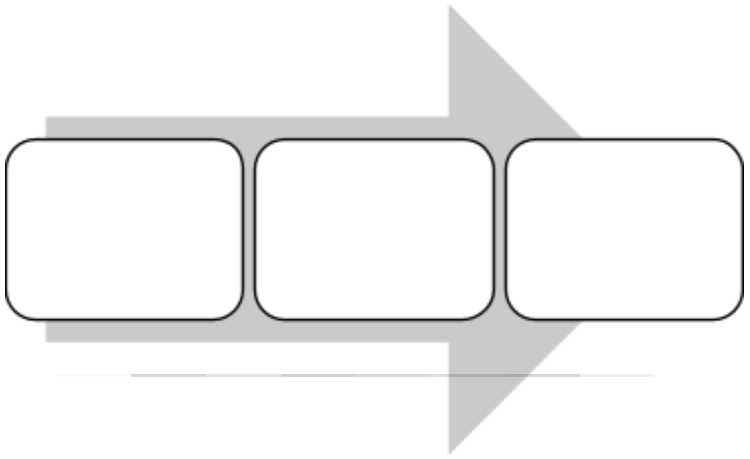

Transportation sector is one the major contributor in the total energy consumed per year worldwide. Global transportation accounts for almost on third of the energy consumed each year [3] and light duty vehicles contribute to more than half of that [4]. A lot of research has been going on how to convert commercial vehicles into ecofriendly and fossil fuel free in order to control CO2 emissions globally.

The two main emerging vehicle technologies in this regard are battery electric vehicles (BEVs) and fuel cell vehicles (FCVs). Whether we should invest our time and money in the development of any one of them is a very critical and future defining decision. Both, battery as well a fuel cell technology (along with hydrogen production) are fairly developed technologies [5, 6] and one cannot be simply discarded on the basis of maturity. One fair way to come up with a definite answer is to analyze both the technologies on an energy efficiency

basis while keeping all the other parameters constant. Hence, in order to know which type of vehicle is more energy efficient a comparison has been made on the basis of energy efficiencies of each operation involved from generation to consumption in the grid to wheel cycle for BEVs and FCVs. Although the FCVs have some advantages over BEVs like faster refueling rate and longer ranges, still the capital cost of an accompanied hydrogen economy is very high and the storage conversion efficiencies of hydrogen are still pretty low.

Although, all the technology or resources required to implement hydrogen economy are already present and a lot of studies [7, 8] have been conducted to identify the costs and technical challenges related to a hydrogen economy. However, these studies fall short on discussing the costs and challenges related to synthesis, delivery, conversion and storage of hydrogen. There are many questions that need to be answered, for instance, what is the maximum efficiency we can achieve for all the processes involved from generation of hydrogen to its usage? How the hydrogen is produced [9]? Is that source green? If water is used in electrolysis for hydrogen synthesis then where would that water come from? How much it would cost to build a hydrogen delivery infrastructure? These and other such questions needs to be answered before we began any efforts towards the development of such an economy. The shortfalls of such an economy are discussed in detail in this paper and it has been proposed that an ‘electric economy’ make far more sense than a ‘hydrogen economy’. Although, environmental impacts of hydrogen economy, cost analyses of BEVs and FCVs and their performance efficiencies have been reported before in the literature but a comparative analysis of their energy efficiencies have been relatively an overlooked area of research and that is why it is the main theme of this research.

4.2 Comparative analysis of BEVs and FCVs

A comparative analysis between BEVs and FCVs can be made by considering each step involved from getting energy from the grid to finally utilizing it. It is a rule of thumb that every operation from generation to consumption in the energy cycle contributes to the overall efficiency and cost. Lesser number of steps probably means greater efficiency at the endpoint. Following is a step by step efficiency calculation for both types of vehicles. As these calculations are more pertinent to a renewable energy future, it is assumed that the electricity utilized to charge batteries or to undergo electrolysis of water is completely renewable.

4.2.1 Efficiency Calculation of Battery Electric Vehicle

The steps involved from grid to wheel of BEV are; generation of electricity through solar photovoltaics, transmission of that electricity through the grid, conversion of AC current to DC current, energy storage in Lithium ion batteries, conversion of DC current back to AC and consumption of electricity by motor to power the vehicle.

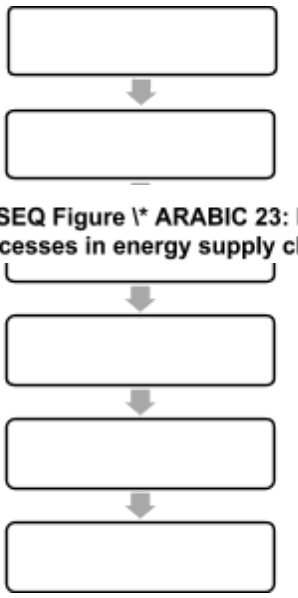

Figure SEQ Figure * ARABIC 23: BEV step by step processes in energy supply chain

For the grid to wheel efficiency calculation of a battery electric vehicle, Tesla Model S is used as a reference [10]. Considering that the electricity we use for charging the batteries comes completely from renewable resources (like solar or wind), we just have to consider the transmission losses in the grid. The grid in United States (considering United States grid as a reference for grid losses) is quite efficient and according to U.S. department of energy the annual average grid losses from 2004 to 2014 were only 5% [11]. The grid provides AC current while the batteries store the charge in DC. So, in order to convert AC to DC we need

a charger. The peak charger efficiency of Tesla Model S charger is around 92% [10]. Moreover, current leakages in Li-ion batteries should also have to be considered. A good estimate for the charging efficiency of a Li-ion battery would be 90% [12]. Tesla model S runs on AC motors, therefore to convert the DC current supplied by the batteries into AC current, an inverter has to be used with roughly an efficiency of 90% [13]. Finally the motor provides the necessary torque to accelerate the car with efficiency close to 95% [14]. The drive train of the car can be considered with losses very close to 0% as the effect of drivetrain efficiency is neutralized as it is used in calculations for energy efficiencies of both types of vehicles in discussion.

Assuming that if the energy suppl 85 KWh (Kilowatt-hour), we can get a good estimate of how much energy we initially need to generate for a battery electric car.

$$X = \frac{a}{(b*c*d*e*f)}$$

Where;

X = energy required

a = Energy consumed by the battery electric car

b = grid efficiency

c = charger efficiency

d = charging efficiency

e = inverter efficiency

f = motor efficiency

$$X = \frac{85\ KWh}{(0.95) * (0.92) * (0.90) * (0.90) * (0.95)}$$

$$X = 126.38\ (\tilde{}126\ KWh)$$

4.2.2 Efficiency Calculation of Fuel Cell Vehicle

The steps involved from grid to wheel of FCV are; generation of electricity through solar photovoltaics, transmission of that electricity through the grid, conversion of AC current to DC current, electrolysis of water, compression/liquefaction of hydrogen, transportation of hydrogen, use of hydrogen in fuel cell, conversion of DC current to AC and consumption of electricity by motor to power the vehicle.

For the grid to wheel efficiency calculation of a Fuel cell vehicle, Honda Clarity or Toyota Mirai is used as reference. Although according to a range of 312 miles [11] of Toyota Mirai 2016 model the total energy consumption of the car would be different from that of Tesla Model S. But just for the ease of calculation it is assumed that the fuel cell car also delivers energy of 85 KWh to the wheels for a particular range. The first step in the grid to wheel cycle of a fuel cell vehicle is the production of hydrogen through electrolysis. Electrolysis requires DC current and hence a charger will be required to convert AC current to DC. The charger efficiency is 92% [10]. The electrolysis step is highly energy intensive process with an overall efficiency of not more than 75% [15]. This hydrogen which is produced through electrolysis cannot be used directly due to very low density and it needs to be

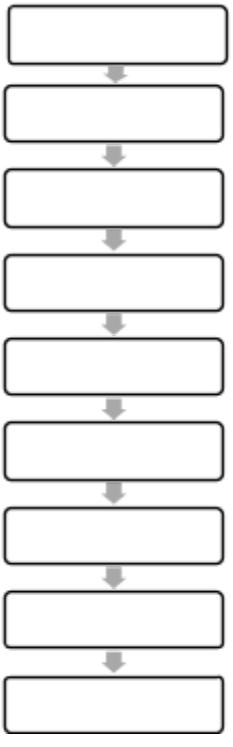

compressed or liquefied. Compression is considered here being less energy intensive than liquefaction [16] and both Toyota Mirai and Honda Clarity use compressed hydrogen [17]. The compression efficiency for hydrogen is 90% [18].

Now the compressed hydrogen is supposed to be transported to hydrogen filling stations in cities or on highways. 80% is a good estimate for transportation efficiency [15, 19]. Once the tank of the car is filled with compressed hydrogen, it will be utilized in the fuel cell to produce current to run the motor according to the variable load conditions. Commercial fuel cells are almost 50% efficient [15]. Again, the DC current produced by the fuel cell needs to be converted to AC through an inverter with an efficiency of 95% [13]. Finally motor can be assumed to have efficiency as previously mentioned which is 95% [14].

Assuming that if the final energy to the wheels is 85 KWh, we can again get a good estimate of how much energy we initially need to generate for a fuel cell car.

$$Y = \frac{g}{(h*i*j*k*l*m)}$$

Where;

Y = energy required

g = energy consumed by the fuel cell car

h = charger efficiency

i = electrolysis efficiency

j = compression efficiency

k = fuel cell efficiency

l = inverter efficiency

m = motor efficiency

$$Y = \frac{85\ KWh}{(0.92) * (0.75) * (0.90) * (0.50) * (0.90) * (0.95)}$$

$$Y = 320.17\ (\tilde{}\ 320\ KWh)$$

Following graph shows the compression energy required to compress hydrogen to desired pressures. Almost 1.12 units of energy are required to compress hydrogen to a pressure of 80 MPa [15]. The data for the graph was taken from the article [15]. HHV refers to higher heating value in the graph.

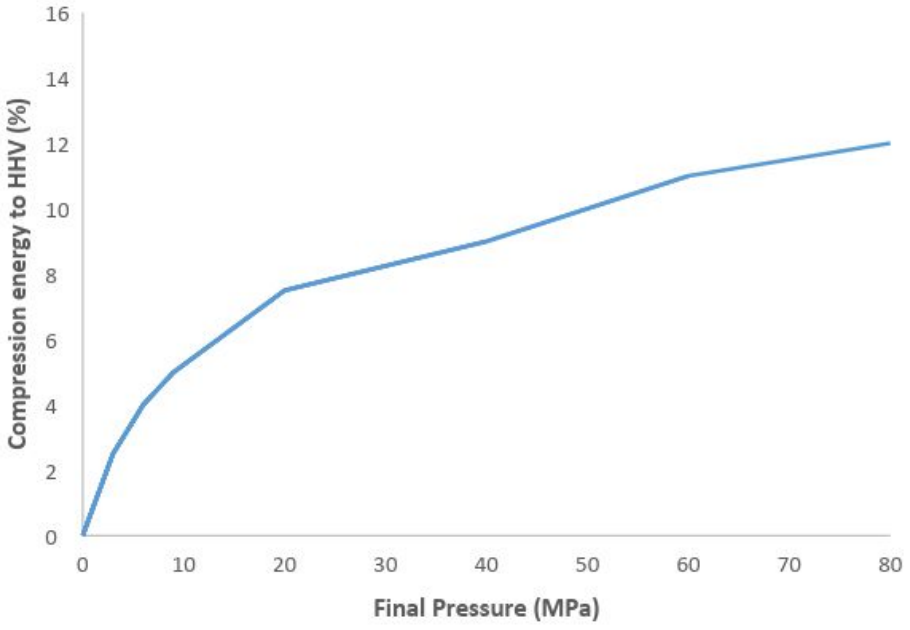

4.3 Result

Now that we have got the energy required initially for both type of cars we can compare them by simply taking the ratio of the energies.

Ratio = Y/X

Ratio = 320/126

Ratio = **2.53**

This ratio clearly shows that the fuel cell vehicle will require 2.5 times more energy than the battery electric vehicle for a similar range.

4.4 Hydrogen Economy and Fuel Cell Vehicles

Considering the above calculations, it seems fair that fuel cell vehicles will ever surpass battery electric vehicles. Apart from the fact that battery electric vehicles require lesser energy than fuel cell vehicles, there are a number of other factors that does not as well support fuel cell vehicles.

Just as we have a well-established infrastructure for fossil fuel based economy, in order to shift towards a hydrogen economy we need to first establish a multi-trillion dollar hydrogen delivery infrastructure [20, 21]. Whereas in the case of battery electric vehicles, there is no need for a new infrastructure as the infrastructure to supply electricity is already present in the form of national grids.

4.4.1 Hydrogen as energy carrier

There is a big misconception with hydrogen being an energy source, when it is just an energy carrier. It is a way to store the energy from natural gas, solar energy, wind, uranium, etc. [10].

The energy storage capability of hydrogen is higher than that of lithium on a per unit mass basis but the volumes required to store hydrogen far surpass any viable limits for acceptable storage on a vehicle based system. Of all the manmade energy sources, hydrogen has the highest specific energy of around 33.3 kWh/kg while lithium based batteries can achieve specific energies of up to 0.55 kWh/kg as shown in Figure 5. The figures, however, for the energy densities of the materials present a different picture where hydrogen when compressed to a pressure of 200 bar has an energy density of 2.37 kWh/dm^3 while lithium ion batteries without the need of any pressurization and owing to the naturally occurring solid state of lithium can show up to 1.69 kWh/dm^3 of energy density [22].

Further energy requirements imposed on the storage of energy using hydrogen because of compression can be resolved by the use of metal hydrides that are capable of chemically storing hydrogen for extended periods of time [23]. The technologies that will enable hydrogen adoption as a widely used fuel are currently in their infancy and therefore require ample time in order to achieve sufficiently higher efficiencies that are needed to compete with batteries.

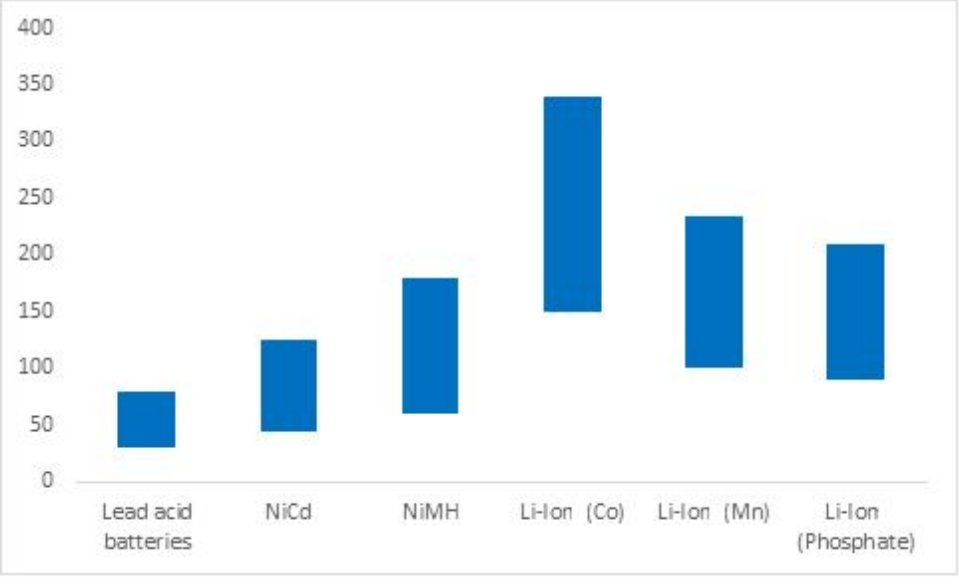

4.4.2 Sources of hydrogen

According to the current situation of energy production in United States [24], 95% of it is produced through steam methane reforming. Methane being a derived product of fossil fuel is more dangerous than carbon dioxide to the ozone and environment. Leakage of the gas does not make it an environmental friendly process. Using hydrogen derived from fossil fuel is just like moving from one addiction to another. There are multiple technologies which are capable of producing hydrogen from multiple sources such as hydrocarbons, water and biomass. Of these technologies, steam reforming, partial oxidation, biomass gasification and alkaline electrolyzer are commercial of which hydrocarbon utilizing steam reforming and partial oxidation have higher efficiencies of between 60-85%. No other technology is capable of achieving such high efficiencies and this is because of the age of these technologies. Following the trend of adoption of renewable technologies for electricity production, hydrogen production is also moving towards renewable means of production which include photolysis, dark fermentation, photo fermentation, thermochemical water splitting and photoelectrochemical water splitting. The ultimate goal of these technologies is to produce hydrogen using the energy of sun or nuclear reactors with higher efficiencies which as of now lie between 0.1-80 percent between these technologies [25, 26].

4.4.3 Economic restraints on hydrogen economy

Fuel cell vehicles and fuel cells are more expensive than battery electric vehicles and battery packs respectively [27, 28]. Being the driving force behind the evolution of hydrogen economy, fuel cells development is essential and is being pursued enthusiastically. Fuel cells will ultimately supply not only electricity but the heating services as well in the envisioned hydrogen economy. The other piece of the puzzle is the creation of a hydrogen production and transport infrastructure and high capital requirements for this purpose are holding back

the spread of the hydrogen economy. Key ideas like gradual phasing out of the fossil fuel based infrastructure and converting to a hydrogen production system are seen as the way forward. Decarbonization of our energy supply is a trend that has already began and switching from coal to liquid fuel to natural gas is the embodiment of the idea. For transport of the fuel, compression and liquefaction are the most common means utilized which require a lot of energy and therefore render the process economically unviable. Building the production infrastructure locally, utilizing a varied energy source provided indigenously is a way to overcome the long distance transfer of hydrogen and allow for the creation of stability and reliability in the hydrogen economy [29].

Hydrogen storage is both difficult and expensive and traditional methods involving gaseous phase storage are highly inefficient thus resulting in excessively short storage times. New technologies for hydrogen revolves around the idea of using solid phase materials which will allow safe storage of hydrogen. Of these technologies, metal hydrides along with carbon structures and glass microspheres are currently the state of the art and are moving steadily towards economic hydrogen storage. Using the stored hydrogen is the last step in the life cycle of the process and fuel cells and gas turbines are used on both large scales as well as in small devices. Manufacturing low cost and high efficiency utilization devices is the last step towards the realization of the hydrogen economy [30].

4.4.4 Hydrogen safety

The flammability range of Hydrogen is extremely wide at between 4 to 75% in the air which is higher as compared to other fuels. This coupled with the minimum combustion initiation energy of just 0.02mJ render hydrogen to be a very dangerous fuel requiring extensive safety measures. Positive aspects associated to hydrogen are its high auto ignition temperature of

585°C and a diffusion rate of 0.61 cm^3/sec which is four times higher than that of methane [31]. Turning hydrogen to an everyday fuel for transportation will also rely on public opinion regarding the safety of the fuel which has already been tainted by the Hindenburg incident. New safety standards need to be developed and practiced and a reliable track record needs to be set for hydrogen safety in order to make hydrogen an acceptable fuel. Current work is focused on dealing with the issues regarding the flammability and buoyancy of the gas as well as its interaction with other gases and other solid materials. Hydrogen embrittlement is a phenomenon which warrants the use of specialized equipment in the handling of the fuel and safety measures need to be taken and multiple redundancies need to be put in place in order to avoid any preventable disaster. Hydrodynamics of hydrogen-air mixtures are being studied to develop procedures for containment and safety of both large scale infrastructure as well as individual human life [30].

4.4.5 Resource based technological restraints

Any scenario that can be envisioned involving the use of either batteries or fuel cell relies on the large-scale production of increasingly efficient units which in turn will rely on the availability of raw materials needed in the manufacturing process. In the case of lithium metal oxide batteries, the active cathode material in use is LiMeO2 where the metal Me is usually Cobalt, Nickel or Manganese. The large-scale production of batteries requires the extraction of these metals from ores which involves different metal refiners which subsequently rely on miners for maintaining a constant supply of these metals. With the increase in demand for rechargeable batteries, the demand for the constituent metals of batteries has also increased. The demand of cobalt alone has increased from 700 to 12000 tons per annum in the decade between 1995 and 2005. In order to cope with the increasing demand and to reduce the environmental impact of the production process, recycling of used

batteries is now being carried out which can reduce the energy requirements 51% when compared to natural resource extraction [32]. Other than the base material, manufacture of a lithium ion battery also requires the use of anode, electrolyte and separator materials which most commonly are graphite powder, lithium salts and organic solvents and microporous membranes respectively. In the current technological state, the cost of lithium ion batteries is higher than lead acid batteries by up to eight times and up to four times as compared to nickel metal hydride (NMH) batteries. But positive forecast for the cost of these batteries is being predicted based on the growth of the market where the cost can decrease from $650 to $325 per kWh form 2009 to 2020 as per the analysis by Deutsche Bank [33]. Further cost analysis based on the production of up to 100,000 electric vehicles packs annually, the cost of a unit lies around $16,596 of which major costs are involved in the labor for cell and pack manufacturing. In the study, the cost of battery components is only 29% of the total cost [34]. Because of the existence of a competitive market and an established supply chain which is complimented by the recycling practices which are becoming increasingly more commonplace, the battery manufacturing sector for electric vehicles is on its way to becoming a viable business model.

While some difficulties being faced in the battery sector include battery management and the establishment of an efficient charging infrastructure, on the other hand fuel cell based electric vehicles are facing more basic problems such as with the high cost of fuel cells, their life cycle and reliability. The contributions being made by companies and some governments in the development of fuel cells is set to boost the technology and allow it to be deployed not only in cars but in micro applications such as cell phones as well. Because they use hydrogen as a fuel, the fuel cell vehicles are technically free of carbon dioxide and can be used as a means of producing electricity for homes in certain cases as well [35]. Proton exchange

membrane fuel cells (PEMFC) are the most suitable technology to be used in an onboard vehicle scenario and therefore the material basis for these cells is under consideration. The main components of a fuel cell are the polymer electrolyte membrane, gas diffusion layer, catalysts for the anode and cathode sides and the bipolar plates. These components collectively form the membrane electrode assembly of the cell which is the core of the cell and determines the efficiency and cost of the entire system [36]. Catalysis is crucial in the performance of a fuel cell and platinum is used widely for this purpose which drives up the cost of the system. Using this expensive noble metal also inhibits the large scale economic roll out of fuel cell technology. The cost of creating fuel cell vehicles lies around $2000/kW and a typical fuel cell vehicle is to consume up to 50kW resulting in a product that is unable to compete with the existing internal combustion engine based vehicles as well as with other technologies like hybrid and battery powered vehicles. Currently the costs of fuel cell components are high and together with the reduction in their cost and increase in the energy density of the cell stack, the cost of manufacture can be reduced to between $15 and $145 per kW based on analysis of different rates of technological advancement. The cost of proton exchange membrane is around $500/$m^2$, platinum requirements are around 2-4g/m^2, electrode cost is $1423/$m^2$, bipolar plate cost is $1650/$m^2$ and the hand assembly costs are $385/kW. These values are expected to reduce drastically in the following years and the technology is therefore expected to become competitive [37].

The trend of moving towards a more carbon free economy and energy mix is apparent and rapidly spreading in the world. Transport sector consumes a huge portion of our energy produced and therefore is a crucial sector to be targeted in the effort to decarbonize. Based on the information provided, battery powered vehicles are ready to not only compete but replace the ICE technology which will open the gateway for the induction of more sustainable

attitudes which will be helpful in the advancement and adoption of fuel cell technology. There is still some time remaining in the growth of fuel cell technology to a level where it can become more prevalent.

4.5 Environmental impact of electric vehicle technologies

For the battery powered vehicles, the impact is based both on the energy requirements of extraction as well as the energy involved in the charging of these batteries. In many measurement cases where parameters like abiotic depletion potential, nonrenewable energy demand and global warming potential, the burden of battery powered vehicles is always lower than that of internal combustion engines [38]. The greenhouse gas emissions associated with the use of fuel cell vehicles is substantially higher than that of battery powered vehicles, hybrid vehicles or conventional ICE. This fact is attributed to the complex extraction and production methods involved in the fuel cell vehicle manufacturing process. On an average the emissions of fuel cell vehicles are around 9800 kg as compared to the 4700 kg emissions of battery powered vehicles [39]. The difference in the levels of emissions is inherent to the source of hydrogen fuel production. Development of sustainable hydrogen production technologies is an unsurmountable obstacle in achieving a decarbonized fuel cell based hydrogen economy.

Battery manufacturing technology is a mature science and has shown steady rise in energy density over the decades, while fuel cells have been hindered by the complication associated with the containment of Hydrogen owing to the gaseous nature of the fuel. This slow pace associated with fuel cell technology is assumed to persist as it has. Therefore, relying on battery power makes much more sense in the present time. Fully utilizing the potential of

lithium as opposed to the potential of hydrogen might yield more productive and user-friendly devices by overcoming the need to store gaseous fuel.

4.6 Conclusion

The impact that the current fossil fuel based energy infrastructure is having on the economy needs to be offset by steering away from using dirty energy and switching to cleaner technologies. Considering the above-mentioned points, it looks like the development and adoption of fuel cells and hydrogen economy is still in the pipeline. Not only the battery electric vehicles are 2.5 times more efficient than their contemporary fuel cell vehicles, as shown through the comparative analysis, but they are also lower in cost, require no new fuel infrastructure, reduce pollution and promise an integrated renewable energy based future.

4.7 References

1. *Repowering Transport Project White Paper.*
2. *REDUCING TRANSPORT GREENHOUSE GAS EMISSIONS TRENDS & DATA 2010*
3. Lynes, M., *International Energy Outlook 2016.* 2016.
4. Frei, C., *Global Transport Scenarios 2050.* 2011.
5. Acres, G.J., *Recent advances in fuel cell technology and its applications.* Journal of Power Sources, 2001. **100**(1): p. 60-66.
6. Scrosati, B., *Recent advances in lithium ion battery materials.* Electrochimica Acta, 2000. **45**(15): p. 2461-2466.
7. *U.S. National Research Council. (2004). The hydrogen economy: Opportunities, costs, barriers, and R&D needs.* 2004.
8. *American Physical Society. (2004, Mar). The Hydrogen Initiative Panel on Public Affairs.* 2004.
9. Shandarr, R., C.A. Trudewind, and P. Zapp, *Life cycle assessment of hydrogen production via electrolysis - a review.* Journal of Cleaner Production, 2014. **85**: p. 151-163.

10. Barbir, F., *Transition to renewable energy systems with hydrogen as an energy carrier.* Energy, 2009. **34**(3): p. 308-312.
11. *Average of annual losses in 2005 through 2014.* 2016.
12. Linden, D., *Handbook of batteries and fuel cells.* New York, McGraw-Hill Book Co., 1984, 1075 p. No individual items are abstracted in this volume., 1984. **1**.
13. Nakashima, S., et al. *Piezoelectric-transformer inverter with maximum-efficiency tracking and dimming control*. in *Applied Power Electronics Conference and Exposition, 2002. APEC 2002. Seventeenth Annual IEEE*. 2002. IEEE.
14. Bonnett, A.H. *An update on ac induction motor efficiency*. in *Petroleum and Chemical Industry Conference, 1993, Record of Conference Papers. The Institute of Electrical and Electronics Engineers Incorporated. Industry Applications Society 40th Annual*. 1993. IEEE.
15. Bossel, U., *Does a hydrogen economy make sense?* Proceedings of the IEEE, 2006. **94**(10): p. 1826-1837.
16. Zhou, L., *Progress and problems in hydrogen storage methods.* Renewable and Sustainable Energy Reviews, 2005. **9**(4): p. 395-408.
17. *Honda FCX Clarity—main specifications.*
18. Matsuda, H. and M. Nagami, *Study of large hydrogen liquefaction process.* 수소에너지, 1997. **8**(3): p. 175-175.
19. *THE HYDROGEN ECONOMY, Opportunities, Costs, Barriers, and R&D Needs.* 2004.
20. Friedemann, A., *Forums Forums-Off Topic Forum FUN> Debate Forums> Political Debate Forum> Very good perspective on.*
21. Dunn, S. and J.A. Peterson, *Hydrogen futures: Toward a sustainable energy system*. Vol. 157. 2001: Worldwatch Institute Washington, DC.
22. Edwards, P.P., et al., *Hydrogen and fuel cells: towards a sustainable energy future.* Energy policy, 2008. **36**(12): p. 4356-4362.
23. Zhang, J., et al., *A review of heat transfer issues in hydrogen storage technologies.* Journal of Heat Transfer, 2005. **127**(12): p. 1391-1399.
24. *HYDROGEN PRODUCTION: NATURAL GAS REFORMING.*
25. Holladay, J.D., et al., *An overview of hydrogen production technologies.* Catalysis today, 2009. **139**(4): p. 244-260.
26. Ni, M., et al., *A review and recent developments in photocatalytic water-splitting using TiO2 for hydrogen production.* Renewable and Sustainable Energy Reviews, 2007. **11**(3): p. 401-425.
27. Bauman, J. and M. Kazerani, *A comparative study of fuel-cell–battery, fuel-cell–ultracapacitor, and fuel-cell–battery–ultracapacitor vehicles.* IEEE Transactions on Vehicular Technology, 2008. **57**(2): p. 760-769.
28. Thomas, C., *Fuel cell and battery electric vehicles compared.* international journal of hydrogen energy, 2009. **34**(15): p. 6005-6020.
29. Wang, M., et al., *The intensification technologies to water electrolysis for hydrogen production–A review.* Renewable and Sustainable Energy Reviews, 2014. **29**: p. 573-588.
30. Barreto, L., A. Makihira, and K. Riahi, *The hydrogen economy in the 21st century: a sustainable development scenario.* International Journal of Hydrogen Energy, 2003. **28**(3): p. 267-284.
31. Conte, M., et al., *Hydrogen economy for a sustainable development: state-of-the-art and technological perspectives.* Journal of Power Sources, 2001. **100**(1): p. 171-187.
32. Rosyid, O.A., D. Jablonski, and U. Hauptmanns, *Risk analysis for the infrastructure of a hydrogen economy.* International Journal of Hydrogen Energy, 2007. **32**(15): p. 3194-3200.
33. Dewulf, J., et al., *Recycling rechargeable lithium ion batteries: critical analysis of natural resource savings.* Resources, Conservation and Recycling, 2010. **54**(4): p. 229-234.
34. *Annual_Report_2009.*

35. Lowe, M., et al., *Lithium-ion batteries for electric vehicles.* Duke University Center on Globalization, Governance and Competitiveness, Tech. Rep., 2010.
36. Chan, C.C., *The state of the art of electric, hybrid, and fuel cell vehicles.* Proceedings of the IEEE, 2007. **95**(4): p. 704-718.
37. Mehta, V. and J.S. Cooper, *Review and analysis of PEM fuel cell design and manufacturing.* Journal of Power Sources, 2003. **114**(1): p. 32-53.
38. Notter, D.A., et al., *Contribution of Li-ion batteries to the environmental impact of electric vehicles*. 2010, ACS Publications.
39. Granovskii, M., I. Dincer, and M.A. Rosen, *Economic and environmental comparison of conventional, hybrid, electric and hydrogen fuel cell vehicles.* Journal of Power Sources, 2006. **159**(2): p. 1186-1193.

Chapter # 5

Hybrid Cathode Materials for Lithium- Air Batteries

5.1 Introduction

With rising energy demand worldwide with an increasing awareness towards global warming, countries are moving towards energy generation resources that are renewable in nature. As most of such renewable resources like solar and wind offers intermittent energy supply, storage of such energy has been a problem. Lithium based batteries appears to be the most promising solution for energy storage [1, 2]. The problem with lithium ion batteries is their low energy densities. Recently, the discovery of lithium air batteries has showed a ray of hope as their practical energy densities are comparable to that of gasoline [3]. Lithium air battery technology is still in its premature stage and it needs improvement in a number of areas. One such area is its oxygen reduction reaction (ORR) and oxygen evolution reaction (OER) kinetics [4]. A typical problem is that the exchange current density at cathode is many times less than that at anode ref. Moreover, voltage efficiency and recharge rate is also quite low in such batteries.

Hence, the need for a redox bi-functional catalyst is necessary for the development of Li-Air batteries. Platinum and Ruthenium offers good performance as ORR and OER catalysts respectively but both of these catalysts have issues like high cost and scarcity [5]. A good alternative is the use of porous materials loaded with transition metals as cathodes for Li-air batteries [6-10], however, it raises the problem of leaching and metal agglomeration [11]. An efficient way to solve this problem is the pyrolysis of metal organic frameworks (MOFs) to derive nano-porous carbon structures doped with heteroatoms, like nitrogen, that can eventually be used as cathode material for Li-air batteries. Different carbon forms like

graphenes and nanotubes have also been showed to offer good ORR activity [12-17]. Cobalt and Manganese oxide offers good performance as a catalysts for metal air batteries [18, 19].

In this study Co-MOF and Fe-MOF derived nano-porous carbon structures that were further hybridized with MnO_2 were tested as cathode materials for Li-Air batteries to analyze their ORR and OER activities. Cyclic voltammetry was performed of these materials at different scan rates under dissolved oxygen and inert conditions to obtain their I-V curves. ORR and OER activity of all the materials was reported to analyze their performance and suitability for Li-Air batteries.

5.2 Experimental

5.2.1 ZIF-67 Synthesis

1.97 g of 2-methylimidazole was dissolved in a 40 ml of 50/50 (v/v %) of ethanol and methanol. 1.746 g of Co $(NO_3)_2.6H_2O$ was mixed with ethanol and methanol mixture keeping the ratios as before. The two solution were then stirred together for 20 minutes and kept at room temperature for 20 hours. After centrifugation, washing and drying a purple precipitate was obtained.

5.2.2 MIL 53 (Fe-MOF) Synthesis

A solution of 1 mmol $FeCl_3$ and 1 mmol Terephthalic acid in 5 ml of Dimethyl Formamide was set for reaction in a Teflon lined autoclave at a temperature of 150°C for 2 hours. Yellow precipitate was obtained after cooling and centrifugation. In order to remove the solvent 1 gm of powder was dispersed in 500 ml of water for a day which was later again centrifuged and dried in vacuum oven. The obtained powder is basically MIL-53 (Fe-MOF).

5.2.3 MOF derived nano-porous carbon synthesis

MOFs were heated to 350°C and were maintained at that temperature for 1.5 hours using a tube furnace. The temperature was then increased to 750°C with a ramp rate of 2°C/min and was sustained at that temperature for 3.5 hours. Furnace was naturally allowed to cool down. An Ar flow was maintained throughout the experiment. The sample was then treated with H_2SO_4, centrifuged, washed and dried.

5.2.4 Nano-porous carbon/MnO_2 hybrids

1 M solution of $KMnO_4$ was prepared in deionized water. Nano-porous carbon particles derived from ZIF-67 were dispersed in the 100 ml of solution using bath sonicator for 15 minutes. The mixture was then stirred for 30 minutes and HCl (30 %) was added drop-wise to the mixture. The mixture was then transferred in to a Teflon lined autoclave and heated in a box furnace at 80 ℃ for 3 hours. The heated suspension was then filtered and washed using ethanol/water mixture and eventually dried in a vacuum oven at 80 ℃ overnight. The dried sample is actually our product (ZIF-67 derived nano-porous carbon and MnO_2 hybrid). Similar steps were followed to form MIL-53 derived nanporous carbon and MnO_2 hybrid.

Below are the SEM images of MnO_2 modified ZCNT and FCNT samples.

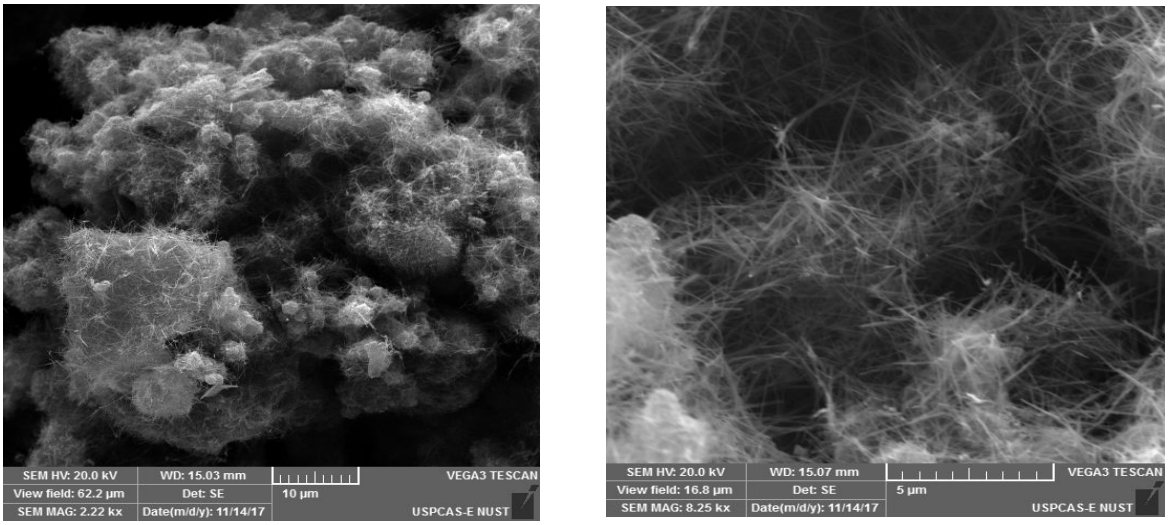

Figure 26. SEM images of ZCNT-M

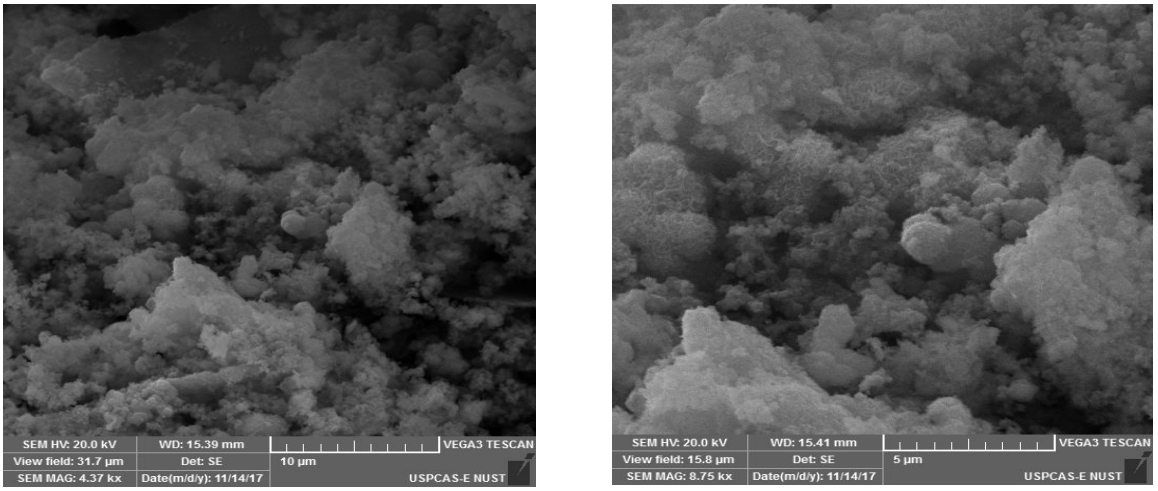

Figure 27. SEM images of FCNT-M

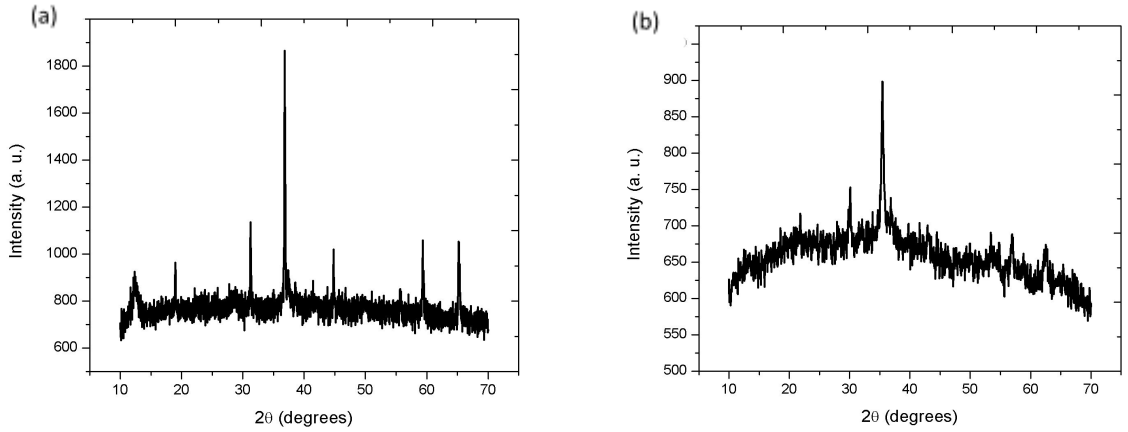

Figure 28. XRD of (a) ZCNT-M and (b) FCNT-M

Figure 28 shows the XRD graphs of ZCNT-M and FCNT-M samples prepared. The graphs were analysed using jade 6.0. The XRD peaks in the sample ZCNT-M were found to be of cobalt oxide (PDF# 43-1003), cobalt carbide (PDF# 43-1144), manganese oxide (PDF# 44-0141) and cobalt manganese oxide (PDF# 32-0297). Whereas the XRD peaks of the sample FCNT-M matches with that of Fe_2C (PDF# 26-0782), Fe_2O_3 (PDF# 39-1346 Maghemite, syn), MnO_2 (PDF# 44-0412, Ramsdellite, syn), and $MnFe_2O_4$ (PDF# 10-0319, Jacobsite, syn). Hence, it proves that samples have actually contain dispersed MnO_2.

5.3 Results and Discussions

All synthesized samples were tested using cyclic voltammetry. 100 µl Ethanol with 20 µl of Nafion were mixed with required sample and mixed thoroughly. Then the slurry was transferred on to a glassy carbon electrode using a micro pipette. The electrode was dried using a hot air blower and then a three electrode system was established. Glassy carbon electrode with our deposited material acted as the working electrode while Ag/AgCl acted as reference and counter electrodes respectively. 0.1 M KOH was used as the electrolyte. Cyclic voltammetry was performed at a scan rate of 100mV/s.

Four prepared samples were tested namely;

- ZIF-67 derived CNTs (ZCNT)
- ZIF-67 derived CNTs/MnO_2 (ZCNT-M)
- MIL-53 derived CNTs (FCNT)
- MIL-53 derived CNTs/MnO_2 Hybrid (FCNT-M)

5.3.1 ZIF-67 derived CNTs/MnO_2 Hybrid

First ZIF-67 derived CNTs (ZCNT) and ZIF-67 derived CNTs/MnO_2 (ZCNT-M) were compared first. To ensure that dissolved oxygen is the only analyte present with in the KOH solution and there are no other analyte species to react with the electrode. The solution was purged with argon gas for 2-3 minutes and then the response was recorded and compared with the solution with dissolved oxygen.

Furthermore, ZCNT was actually compared with ZCNT-M to obtain the values of peak current density, onset potential and peak potentials for oxygen reduction and oxygen evolution reactions.

Figure 30. OER & ORR potential for ZCNT & ZCNT-M

The OER and ORR performance of ZCNT-M is much better than ZCNT. The addition of MnO_2 has markedly increased the current densities roughly by 700%. The increased current densities can be attributed to good catalytic ORR and OER activity of MnO_2. Moreover, a decrease in the onset and peak potentials was also observed for ZCNT-M as compared to ZCNT sample.

Table 3. Onset potentials, Peak Potentials and Current densities

	Onset Potential vs. Ag/AgCl (V)		Peak Potential vs. Ag/AgCl (V)		Peak Current Density (mA/cm^2)	
	OER	ORR	OER	ORR	OER	ORR
ZCNT	0.3	-0.34	0.7	-0.76	1.04	1.44
ZCNT-M	0.1	-0.22	0.6	-0.7	6.38	6.56

Furthermore, the kinetics of ORR and OER reactions were found to be diffusion controlled. A plot between square root of scan rate and peak current density was made for ZCNT-M and diffusion coefficients were calculated using the Randles-Sevcik equation.

$$Ip = 0.4463nFAC\sqrt{\frac{nFvD}{RT}}$$

Table 4. Diffusion Coefficients for ZCNT-M

D_{OER}	$2.4x10^{-4}$ cm^2/s
D_{ORR}	$6.6x10^{-4}$ cm^2/s

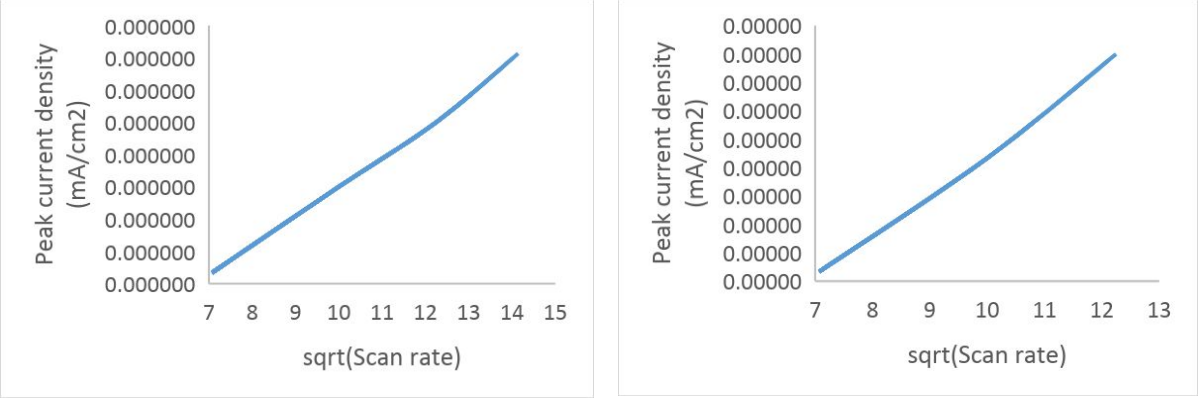

Figure 31. OER and ORR Scan rate vs. Current density

Finally, to analyze the trend of overpotential with the current density, Tafel plots were made. Tafel plots were then used to calculate the exchange current densities.

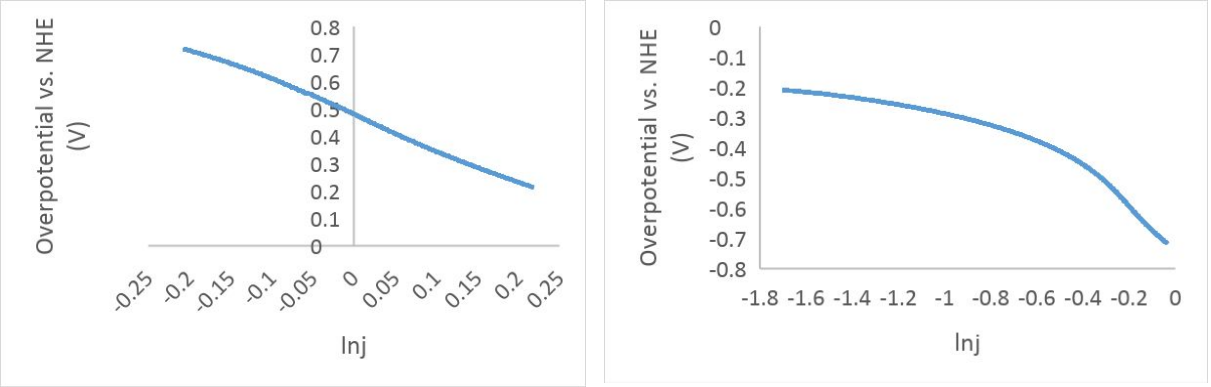

Figure 32. ORR and OER Tafel plots

	Exchange Current density (j^o) (A/cm^2)
ZCNT-M $_{OER}$	$1.46\ x10^{-3}$
ZCNT-M $_{ORR}$	$1.49\ x10^{-3}$

Moreover, CV of ZCNT-M was performed at different scan rates to check its reversibility. A slight shift in peaks was observed which indicated a bit irreversibility.

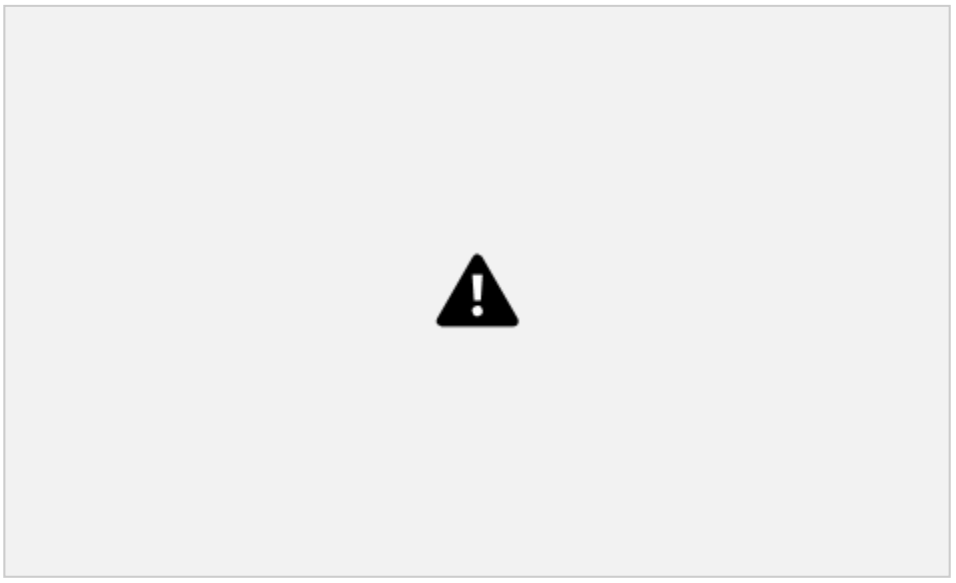

Figure 33. Peak Shift with increasing scan rates

5.3.2 MIL-53 derived CNT/MnO_2 Hybrid

As we did before, in this experiment MIL-53 derived CNTs (FCNT) and MIL-53 derived CNTs /MnO_2 (FCNT-M) were compared first. To ensure that dissolved oxygen is the only analyte present with in th KOH solution and there are no other analyte species to react with the electrode. The solution was purged with argon gas for 2-3 minutes and then the response was recorded and compared with the solution with dissolved oxygen.

Furthermore, FCNT was actually compared with FCNT-M to obtain the values of peak current density, onset potential and peak potentials for oxygen reduction and oxygen evolution reactions.

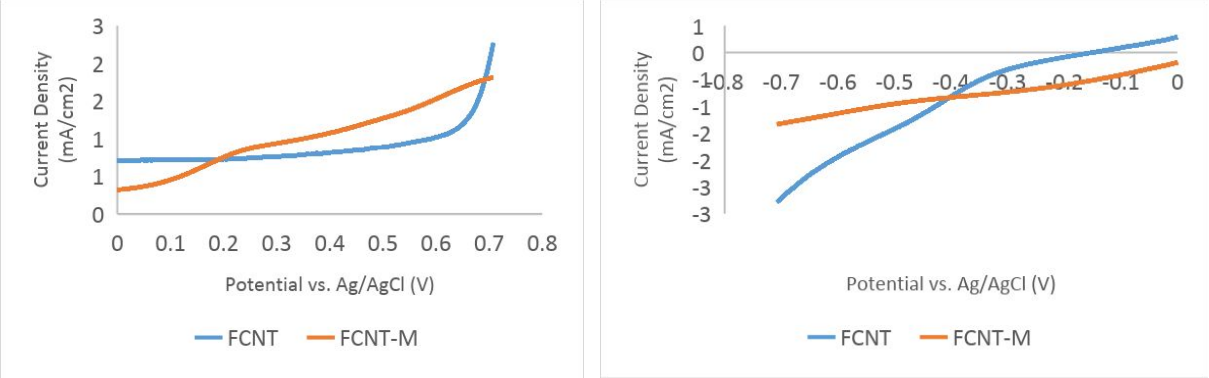

Figure 35. OER & ORR potential for FCNT & FCNT-M

The OER and ORR performance of FCNT-M is much better than FCNT. The addition of MnO_2 has markedly increased the current densities roughly by 200%. The increased current densities can be attributed to good catalytic ORR and OER activity of MnO_2. Moreover, a decrease in the onset and peak potentials was also observed for FCNT-M as compared to FCNT sample.

Table 3. Onset potentials, Peak Potentials and Current densities

	Onset Potential vs. Ag/AgCl (V)		Peak Potential vs. Ag/AgCl (V)		Peak Current Density (mA/cm^2)	
	OER	ORR	OER	ORR	OER	ORR
FCNT	0.55	-0.32	1.0	No peak	17.24	No peak
FCNT-M	0.09	-0.17	0.84	0.93	3.14	3.64

Furthermore, the kinetics of ORR and OER reactions were found to be diffusion controlled. A plot between square root of scan rate and peak current density was made for FCNT-M and diffusion coefficients were calculated using the Randles-Sevcik equation.

$$Ip = 0.4463nFAC\sqrt{\frac{nFvD}{RT}}$$

Table 4. Diffusion Coefficients for FCNT-M

D_{OER}	4.18×10^{-5} cm^2/s
D_{ORR}	2.02×10^{-4} cm^2/s

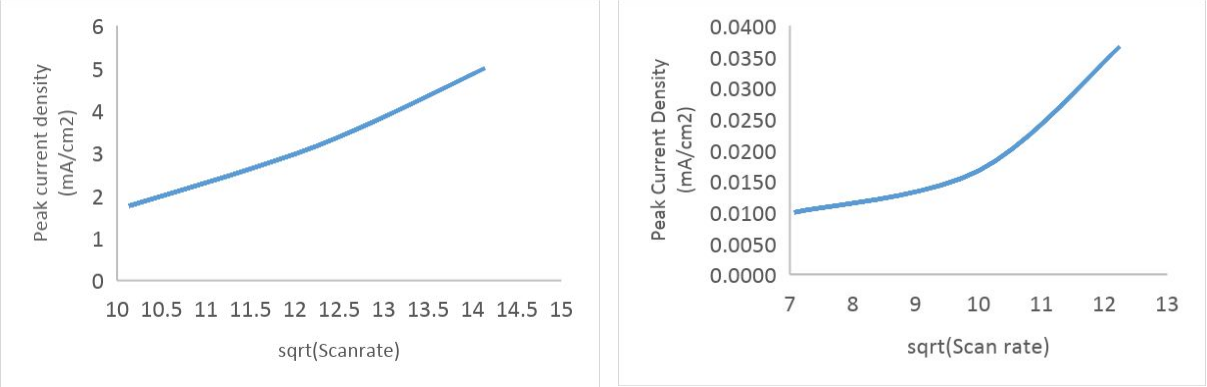

Figure 36. OER and ORR Scan rate vs. Current density

Finally, to analyze the trend of overpotential with the current density, Tafel plots were made. Tafel plots were then used to calculate the exchange current densities.

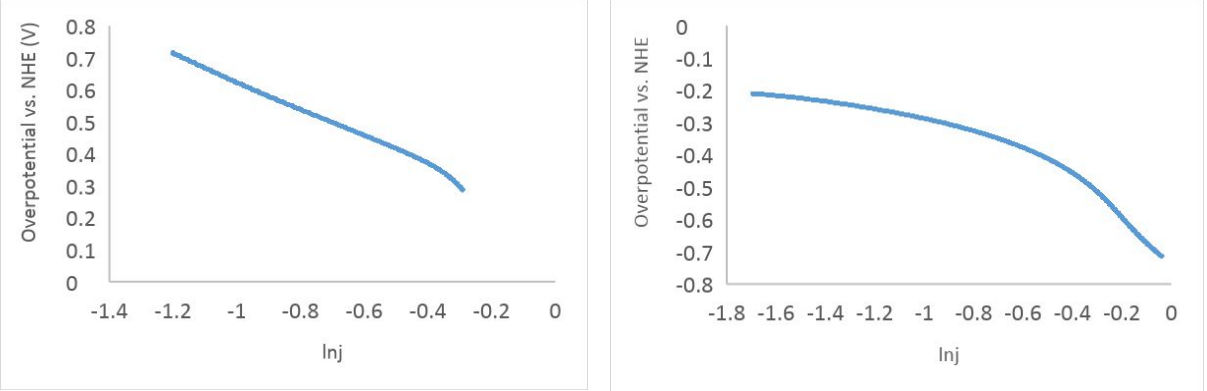

Figure 37. ORR and OER Tafel plots

	Exchange Current density (j^o) (A/cm^2)
FCNT-M $_{OER}$	1.44×10^{-3}
FCNT-M $_{ORR}$	1.53×10^{-3}

Moreover, CV of FCNT-M was performed at different scan rates to check its reversibility. A slight shift in peaks was observed which indicated a bit irreversibility.

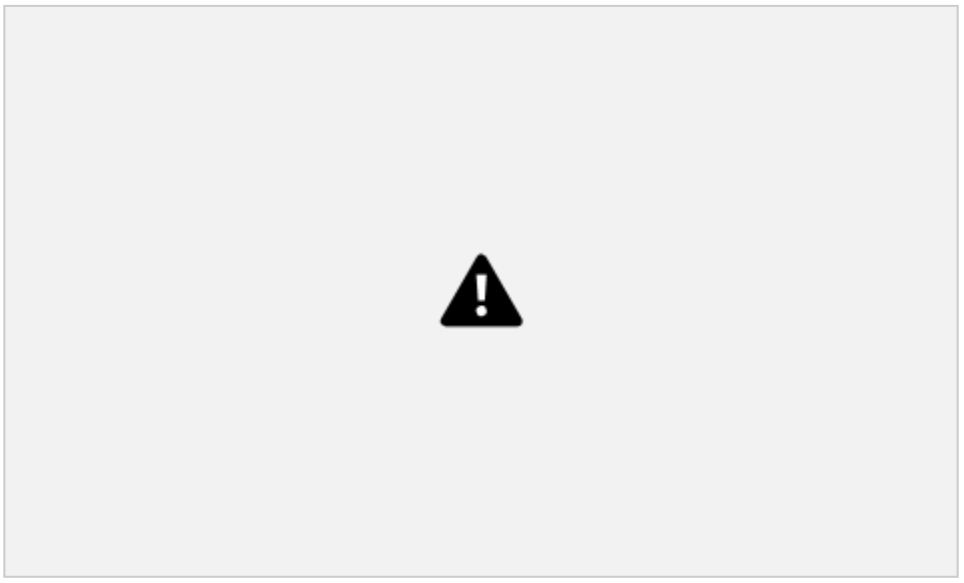

Figure 38. Peak Shift with increasing scan rates

5.4 Conclusion

Conclusively, we can surely say that the in all of the four materials the kinetics is diffusion controlled. The samples modified with MnO_2 do show a marked improvement in terms of lower onset and peak potentials. The reactions are quasi reversible as there is a slight peak shift with increased scan rate. Diffusion coefficients were also calculated which lie in a reasonable limit. ZCNT-M showed an increase in peak current density than ZCNT. The OER peak current density of FCNT-M s quite lower than that of FCNT but FCNT-M also showed ORR activity while FCNT only showed OER activity. We can say that the modified materials are a good and viable alternative for platinum based bi-functional catalysts used for OER and ORR activity as Li-Air battery cathodes because the exchange current densities of the samples are comparable to that of platinum based electrodes although onset potentials are a little higher than Pt electrodes.

5.5 References

[1] J. Liu, Y. Wen, P.A. Van Aken, J. Maier, Y. Yu, Facile synthesis of highly porous Ni-Sn intermetallic microcages with excellent electrochemical performance for lithium and sodium storage, Nano Lett. 14 (2014) 6387–6392.

[2] J. Liu, P. Kopold, C. Wu, P.A. Van Aken, J. Maier, Y. Yu, Uniform yolk-shell Sn4P3@C nanospheres as high-capacity and cycle-stable anode materials for sodium-ion batteries, Energy Environ. Sci. 8 (2015) 3531–3538.

[3] Girishkumar, G., et al. "Lithium− air battery: promise and challenges." *The Journal of Physical Chemistry Letters* 1.14 (2010): 2193-2203.

[4] Shao, Yuyan, et al. "Electrocatalysts for nonaqueous lithium–air batteries: status, challenges, and perspective." *Acs Catalysis* 2.5 (2012): 844-857.

[5] Lee, Youngmin, et al. "Synthesis and activities of rutile IrO2 and RuO2 nanoparticles for oxygen evolution in acid and alkaline solutions." *The journal of physical chemistry letters*3.3 (2012): 399-404.

[6] Wang, Yongcheng, et al. "Reduced mesoporous Co3O4 nanowires as efficient water oxidation electrocatalysts and supercapacitor electrodes." *Advanced Energy Materials* 4.16 (2014).

[7] Fan, Xiujun, et al. "M3C (M: Fe, Co, Ni) nanocrystals encased in graphene nanoribbons: An active and stable bifunctional electrocatalyst for oxygen reduction and hydrogen evolution reactions." *ACS nano* 9.7 (2015): 7407-7418.

[8] Deng, Dehui, et al. "Iron encapsulated within pod-like carbon nanotubes for oxygen reduction reaction." *Angewandte Chemie International Edition* 52.1 (2013): 371-375.

[9] Zhang, Genqiang, et al. "General Formation of Complex Tubular Nanostructures of Metal Oxides for the Oxygen Reduction Reaction and Lithium-Ion Batteries." *Angewandte Chemie* 125.33 (2013): 8805-8809.

[10] Ma, Tian Yi, et al. "Metal–organic framework derived hybrid Co3O4-carbon porous nanowire arrays as reversible oxygen evolution electrodes." *Journal of the American Chemical Society* 136.39 (2014): 13925-13931.

[11] Zhao, Juan, et al. "Performance and stability of Pd–Pt–Ni nanoalloy electrocatalysts in proton exchange membrane fuel cells." *Journal of Power Sources* 196.10 (2011): 4515-4523.

[12] Chen, Sheng, et al. "Nitrogen and Oxygen Dual-Doped Carbon Hydrogel Film as a Substrate-Free Electrode for Highly Efficient Oxygen Evolution Reaction." *Advanced Materials* 26.18 (2014): 2925-2930.

[13] Ma, Tian Yi, et al. "Graphitic carbon nitride nanosheet–carbon nanotube three-dimensional porous composites as high-performance oxygen evolution electrocatalysts." *Angewandte Chemie International Edition* 53.28 (2014): 7281-7285.

[14] Gong, Kuanping, et al. "Nitrogen-doped carbon nanotube arrays with high electrocatalytic activity for oxygen reduction." *science* 323.5915 (2009): 760-764.

[15] Yang, Shubin, et al. "Efficient synthesis of heteroatom (N or S)-doped graphene based on ultrathin graphene oxide-porous silica sheets for oxygen reduction reactions." *Advanced Functional Materials* 22.17 (2012): 3634-3640.

[17] Zhang, Jintao, et al. "A metal-free bifunctional electrocatalyst for oxygen reduction and oxygen evolution reactions." *Nature nanotechnology* 10.5 (2015): 444-452.

[18] Cheng, H., and K. Scott. "Carbon-supported manganese oxide nanocatalysts for rechargeable lithium–air batteries." *Journal of Power Sources* 195.5 (2010): 1370-1374.

[19] Lee, Jang-Soo, et al. "Metal–air batteries with high energy density: Li–air versus Zn–air." *Advanced Energy Materials* 1.1 (2011): 34-50.

Proposed Future Work

Using the nano-wired particles, thermo-responsive polymer switching composite material should be synthesized using polyethylene as the base and nanowires as the filler. Resistances of the composites should be plotted against time and temperature to understand the switching behavior of the as fabricated materials. Once tested, the material should be incorporated with in an actual Li-ion cell to check its performance.

Moreover, the same battery with the quantum composite installed can be simulated on COMSOL Multiphysics of ANYSYS to better understand the heat transfer and thermal runaway behavior of the battery.

Lastly, regarding the hybrid materials for Li-Air batteries, the as synthesized hybrid cathode materials should be used to make actual coin cells. The performance of such coin cells should also be tested to understand the behavior of the material with in a cell.

Journal Papers

- **"Anatomization of the prospects of a Hydrogen Economy in the backdrop of grid to wheel energy efficiency analysis of Battery and Fuel Cell powered Vehicles"**
  Usman Salahuddin, Naseem Iqbal, Haider Ejaz | International Journal of Energy Research

- **"Synthesis of copper oxide nanowires with an emphasis on analysing the effect of oxidation time on the growth of nanowires"**
  Usman Salahuddin, Naseem Iqbal, Humaira Asghar | Material Research Bulletin

- **"Modification of spherical copper particles into nano-wired copper particles: an approach to improve electrical conductivity of thermo-responsive polymer switching material to be used in Li-ion batteries for the improvement of battery safety parameter"**
  Usman Salahuddin, Naseem Iqbal, Humaira Asghar, Haider Ejaz | Bulletin of Materials Science